

Attacks Which Do Not Kill Training Make Adversarial Learning Stronger

Jingfeng Zhang^{*†1}, Xilie Xu^{*2}, Bo Han^{3 4}, Gang Niu⁴, Lizhen Cui⁵,
Masashi Sugiyama^{4 6}, and Mohan Kankanhalli¹

¹Department of Computer Science, School of Computing, National University of Singapore, Singapore

²Taishan College, Shandong University, Jinan, China

³Department of Computer Science, Hong Kong Baptist University, Hong Kong

⁴RIKEN Center for Advanced Intelligence Project, Tokyo, Japan

⁵Joint SDU-NTU Centre for Artificial Intelligence Research (C-FAIR), Shandong University, Jinan, China

⁶University of Tokyo, Tokyo, Japan

Abstract

Adversarial training based on the *minimax* formulation is necessary for obtaining *adversarial robustness* of trained models. However, it is conservative or even pessimistic so that it sometimes hurts the *natural generalization*. In this paper, we raise a fundamental question—do we have to trade off natural generalization for adversarial robustness? We argue that adversarial training is to employ confident adversarial data for updating the current model. We propose a novel approach of *friendly adversarial training* (FAT): rather than employing most adversarial data maximizing the loss, we search for least adversarial (i.e., friendly adversarial) data minimizing the loss, among the adversarial data that are confidently misclassified. Our novel formulation is easy to implement by just stopping the most adversarial data searching algorithms such as PGD (projected gradient descent) early, which we call *early-stopped PGD*. Theoretically, FAT is justified by an upper bound of the adversarial risk. Empirically, early-stopped PGD allows us to answer the earlier question negatively—adversarial robustness can indeed be achieved without compromising the natural generalization.

1 Introduction

Safety-critical nature of some areas such as medicine [1] and automatic driving [2], necessitates the need for deep neural networks (DNNs) to be adversarially robust that generalize well. Recent research focuses on improving their robustness mainly by two defense approaches, i.e., certified defense and empirical defense. Certified defense tries to learn provably robust DNNs against norm-bounded (e.g., ℓ_2 and ℓ_∞) perturbations [3, 4, 5, 6, 7, 8, 9]. Empirical defense incorporates adversarial data into the training process [10, 11, 12, 13, 14, 15]. For instance, empirical defense has been used to train Wide ResNet [16] with natural data and its adversarial variants to make the trained network robust against strong adaptive attacks [17, 18]. This paper belongs to the empirical defense category.

Existing empirical defense methods formulate the adversarial training as a minimax optimization problem (Eq. (2) in Section 2.1) [11]. To conduct this minimax optimization, projected gradient descent (PGD) is a common method to generate the most adversarial data that maximizes the loss,

^{*}Equal Contributions.

[†]Preliminary work was done during an internship at RIKEN AIP.

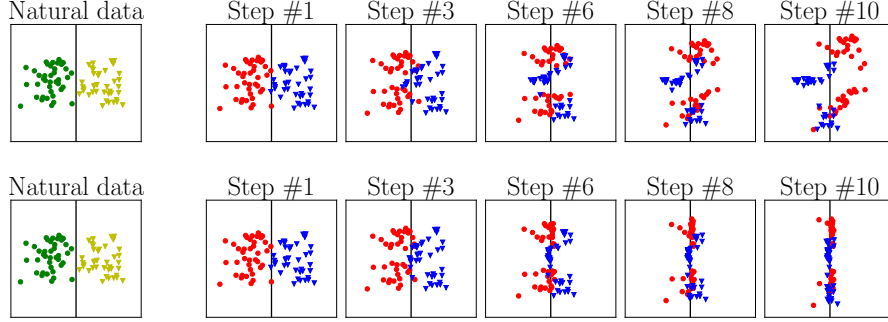


Figure 1: Green circles and yellow triangles are natural data for binary classification. Red circles and blue triangles are adversarial variants of green circles and yellow triangles, respectively. Black solid line is the decision boundary representing the current classifier. Top: the adversarial data generated by PGD. Bottom: the adversarial data generated by early-stopped PGD.

updating the current model. PGD perturbs the natural data for a fixed number of steps with small step size. After each step of perturbation, PGD projects the adversarial data back onto the ϵ -norm ball of the natural data.

However, this minimax formulation is conservative (or even pessimistic), such that it sometimes hurts the natural generalization [19]. For example, the top panels in Figure 1 show that at step #6 to #10 in PGD, the adversarial variants of the natural data significantly cross over the decision boundary and are located at their peer’s (natural data) area. Since adversarial training aims to fit natural data and its adversarial variants simultaneously, such cross-over mixture makes adversarial training extremely difficult. Therefore, the most adversarial data generated by the PGD-10 (i.e., step #10 in top panels) directly “kill” the training, thus rendering the training unsuccessful.

Inspired by philosopher Friedrich Nietzsche’s quote “*that which does not kill us makes us stronger*”, we propose *friendly adversarial training* (FAT): rather than employing the most adversarial data, we search for the least adversarial (i.e., friendly adversarial) data minimizing the loss, among the adversarial data that are confidently misclassified by the current model. We design the learning objective of FAT (Section 3.1) and theoretically justify it by deriving an upper bound of the adversarial risk (Section 3.2). Essentially, FAT considers the model prediction on adversarial data. The aim is to train DNN by the wrongly-predicted adversarial data minimizing the loss and the correctly-predicted adversarial data maximizing the loss.

FAT is a reasonable strategy due to two reasons. It removes the existing inconsistency between attack and defense. Moreover, it adheres to the spirit of curriculum learning. First, the ways of generating adversarial data by adversarial attackers and adversarial defense methods are inconsistent. Adversarial attacks [20, 18, 17] aim to find the adversarial data (not maximizing the loss) to confidently fool the model. On the other hand, existing adversarial defense methods generate the most adversarial data that maximize the loss. These two should be harmonized. Second, the curriculum learning strategy has been shown to be effective [21]. Fitting most adversarial data initially makes the learning extremely difficult, sometimes even killing the training. Instead, FAT learns initially from the least adversarial data and progressively utilizes increasingly adversarial data.

FAT is easy to implement by just early stopping most-adversarial-data searching algorithms such as PGD, which we call early-stopped PGD (Section 4.1). Once adversarial data is misclassified by the current model, we stop the PGD iterations early. Early-stopped PGD has the benefit of alleviating the cross-over mixture problem. For example, as shown in the bottom panels of Figure 1, adversarial data generated by early-stopped PGD will not be located at their peer areas (extensive details in Section 4.2). Thus, it will not hurt the generalization ability much. In addition, FAT based on early-stopped PGD progressively employs stronger and stronger adversarial data (with more PGD steps) engendering increasingly enhanced robustness of the model over the training progression (Section 5.3). This implies that attacks that do not kill the training indeed make the adversarial learning stronger.

FAT has following benefits. (a) conventional adversarial training, e.g., standard adversarial training [11], TRADES [13] and MART [15], can also be modified to be compatible with FAT (Section 5). (b) Compared to conventional adversarial training, FAT has a better standard accuracy for natural data, while keeping a competitively robust accuracy for adversarial data (Sections 5.1 and 6.2). (c) FAT is computationally efficient due to early stopped PGD (Section 5.2). (d) FAT enables larger values of the perturbation bound, i.e., ϵ in Eq. (1) (Section 6.1).

2 Standard Adversarial Training

Let (\mathcal{X}, d_∞) be the input feature space \mathcal{X} with the infinity distance metric $d_{\text{inf}}(x, x') = \|x - x'\|_\infty$, and

$$\mathcal{B}_\epsilon[x] = \{x' \in \mathcal{X} \mid d_{\text{inf}}(x, x') \leq \epsilon\} \quad (1)$$

be the closed ball of radius $\epsilon > 0$ centered at x in \mathcal{X} .

2.1 Learning Objective

Given a dataset $S = \{(x_i, y_i)\}_{i=1}^n$, where $x_i \in \mathcal{X}$ and $y_i \in \mathcal{Y} = \{0, 1, \dots, C-1\}$, the objective function of standard adversarial training [11] is

$$\min_{f \in \mathcal{F}} \frac{1}{n} \sum_{i=1}^n \left\{ \max_{\tilde{x} \in \mathcal{B}_\epsilon[x_i]} \ell(f(\tilde{x}), y_i) \right\}, \quad (2)$$

where \tilde{x} is the adversarial data within the ϵ -ball centered at x , $f(\cdot) : \mathcal{X} \rightarrow \mathbb{R}^C$ is a score function, and the loss function $\ell : \mathbb{R}^C \times \mathcal{Y} \rightarrow \mathbb{R}$ is a composition of a base loss $\ell_B : \Delta^{C-1} \times \mathcal{Y} \rightarrow \mathbb{R}$ (e.g., the cross-entropy loss) and an inverse link function $\ell_L : \mathbb{R}^C \rightarrow \Delta^{C-1}$ (e.g., the soft-max activation), in which Δ^{C-1} is the corresponding probability simplex—in other words, $\ell(f(\cdot), y) = \ell_B(\ell_L(f(\cdot)), y)$.

For the sake of conceptual consistency, the objective function (i.e., Eq. (2)) can also be re-written as

$$\min_{f \in \mathcal{F}} \frac{1}{n} \sum_{i=1}^n \ell(f(\tilde{x}_i), y_i), \quad (3)$$

where

$$\tilde{x}_i = \arg \max_{\tilde{x} \in \mathcal{B}_\epsilon[x_i]} \ell(f(\tilde{x}), y_i). \quad (4)$$

It means alternating the optimization of the deep neural network, with one step maximizing loss to find adversarial data and one step minimizing loss on adversarial data w.r.t. the network parameters θ .

2.2 Projected Gradient Descent (PGD)

To generate adversarial data, standard adversarial training uses PGD to approximately solve the inner maximization of Eq. (4) [11].

PGD formulates the problem of finding adversarial data as a constrained optimization problem. Namely, given a starting point $x^{(0)} \in X$ and step size $\alpha > 0$, PGD works as follows:

$$x^{(t+1)} = \Pi_{\mathcal{B}_\epsilon[x^{(0)}]}(x^{(t)} + \alpha \text{sign}(\nabla_{x^{(t)}} \ell(f_\theta(x^{(t)}), y))), \forall t \geq 0 \quad (5)$$

until a certain stopping criterion is satisfied. For example, the criterion can be a fixed number of iterations K , namely the PGD- K algorithm [11, 15]. In Eq. (5), ℓ is the loss function in Eq. (4); $x^{(0)}$ refers to natural data or natural data corrupted by a small Gaussian or uniform random noise; y is the corresponding label for natural data; $x^{(t)}$ is adversarial data at step t ; and $\Pi_{\mathcal{B}_\epsilon[x^{(0)}]}(\cdot)$ is the projection function that projects the adversarial data back into the ϵ -ball centered at $x^{(0)}$ if necessary.

There are also other ways to generate adversarial data, e.g., the fast gradient signed method [20, 10], the CW attack [18] and Hamming distance method [22].

PGD adversarial training. Besides the standard adversarial training, several improvements to PGD adversarial training have also been proposed, such as Lipschitz regularization [23, 24, 25, 26], curriculum adversarial training [12, 14], computationally efficient adversarial learning [27, 28, 29] and adversarial training by utilizing unlabeled data [30, 31, 32]. In addition, TRADES [13] and MART [15] are also effective adversarial training methods, which trains on both natural data x and adversarial data \tilde{x} (the learning objectives are reviewed in Appendices D.1 and E.1 respectively).

3 Friendly Adversarial Training

In this section, we develop a novel learning objective for friendly adversarial training (FAT). Theoretically, we justify FAT by deriving a tight upper bound of the adversarial risk.

3.1 Learning Objective

Let $\rho > 0$ be a margin such that our adversarial data would be misclassified with a certain amount of confidence.

The outer minimization still follows Eq. (3). However, instead of generating \tilde{x}_i via inner maximization, we generate \tilde{x}_i as follows:

$$\begin{aligned} \tilde{x}_i &= \arg \min_{\tilde{x} \in \mathcal{B}_\epsilon[x_i]} \ell(f(\tilde{x}), y_i) \\ \text{s.t. } &\ell(f(\tilde{x}), y_i) - \min_{y \in \mathcal{Y}} \ell(f(\tilde{x}), y) \geq \rho. \end{aligned}$$

Note that the operator $\arg \max$ in Eq. (4) is replaced with $\arg \min$ here, and there is a constraint on the margin of loss values (i.e., the misclassification confidence).

The constraint firstly ensures $y_i \neq \arg \min_{y \in \mathcal{Y}} \ell(f(\tilde{x}), y)$ or \tilde{x} is misclassified, and secondly ensures for \tilde{x} the wrong prediction is better than the desired prediction y_i by at least ρ in terms of the loss value. Among all such \tilde{x} satisfying the constraint, we select the one minimizing $\ell(f(\tilde{x}), y_i)$. Namely, we minimize the adversarial loss given that some confident adversarial data has been found. This \tilde{x}_i could be regarded as a “friend” among the adversaries, which is termed *friendly adversarial data*.

3.2 Upper Bound on Adversarial Risk

In this subsection, we derive a tight upper bound on the adversarial risk, and provide our analysis for adversarial risk minimization. Let X and Y represent random variables. We employ the definition of the adversarial risk given by [13], i.e., $\mathcal{R}_{\text{rob}}(f) := \mathbb{E}_{(X,Y) \sim \mathcal{D}} \mathbb{1}\{\exists X' \in \mathcal{B}_\epsilon[X] : f(X') \neq Y\}$.

Theorem 1. For any classifier f , any non-negative surrogate loss function ℓ which upper bounds the 0/1 loss, and any probability distribution \mathcal{D} , we have

$$\mathcal{R}_{\text{rob}}(f) \leq \underbrace{\mathbb{E}_{(X,Y) \sim \mathcal{D}} \ell(f(X), Y)}_{\text{For standard test accuracy}} + \underbrace{\mathbb{E}_{(X,Y) \sim \mathcal{D}, X' \in \mathcal{B}_\epsilon[X, \epsilon]} \ell^*(f(X'), Y)}_{\text{For robust test accuracy}},$$

where

$$\ell^* = \begin{cases} \min \ell(f(X'), Y) + \rho, & \text{if } f(X') \neq Y, \\ \max \ell(f(X'), Y), & \text{if } f(X') = Y. \end{cases}$$

Note that ρ is the small margin such that friendly adversarial data would be misclassified with a certain amount of confidence. The proof is in Appendix A.2. From Theorem 1, our upper bound on the adversarial risk is tighter than that of conventional adversarial training, e.g., [13] and [11], where they maximize the loss regardless of model prediction, i.e., $\ell^* = \max \ell(f(X'), Y)$. By contrast, our bound takes the model prediction into consideration. When the model makes correct prediction on adversarial data X' (i.e., $f(X') = Y$), we still maximize the loss; while the model makes wrong prediction on adversarial data X' (i.e., $f(X') \neq Y$), we minimize the inner loss by violation of a

small constant ρ . To better understand the nature of adversarial training and Theorem 1, we provide supporting schematics in Figures 7 and 8 in Appendix A.2.

Minimizing the adversarial risk based on our upper bound aids in fine-tuning the decision boundary using friendly adversarial data. On one side, the wrongly-predicted adversarial data have a small distance ρ (in term of the loss value) from the decision boundary (e.g., Step #10 panels at the bottom series in Figure 1) so that it will not cause the severe issue of cross-over mixture but fine-tunes the decision boundary. On the other side, correctly-predicted adversarial data maintain the largest distance (in term of maximizing the loss value) from their natural data so that the decision boundary is kept far away.

4 Key Component of FAT

To search friendly adversarial data, we design an efficient early-stopped PGD algorithm called PGD- K - τ (Section 4.1), which could alleviate the cross-over mixture problem (Section 4.2) and also aid adversarial training. Note that besides PGD- K - τ , there are other ways to search for friendly adversarial data. We show one example in Appendix B.

4.1 PGD- K - τ Algorithm

Algorithm 1 PGD- K - τ

Input: data $\mathbf{x} \in \mathcal{X}$, label $y \in \mathcal{Y}$, model f , loss function ℓ , maximum PGD step K , step τ , perturbation bound ϵ , step size α
Output: $\tilde{\mathbf{x}}$
 $\tilde{\mathbf{x}} \leftarrow \mathbf{x}$
while $K > 0$ **do**
 if $\arg \min_i f(\tilde{\mathbf{x}}) \neq y$ and $\tau = 0$ **then**
 break
 else if $\arg \min_i f(\tilde{\mathbf{x}}) \neq y$ **then**
 $\tau \leftarrow \tau - 1$
 end if
 $\tilde{\mathbf{x}} \leftarrow \Pi_{\mathcal{B}[\mathbf{x}, \epsilon]}(\alpha \text{sign}(\nabla_{\tilde{\mathbf{x}}} \ell(f(\tilde{\mathbf{x}}), y)) + \tilde{\mathbf{x}})$
 $K \leftarrow K - 1$
end while

In Algorithm 1, $\Pi_{\mathcal{B}[\mathbf{x}, \epsilon]}$ is the projection operator that projects adversarial data $\tilde{\mathbf{x}}$ onto the ϵ -norm ball centered at \mathbf{x} , and $\arg \min_i f(\tilde{\mathbf{x}})$ returns the predicted label of adversarial data $\tilde{\mathbf{x}}$, where $f(\tilde{\mathbf{x}}) = (f^i(\tilde{\mathbf{x}}))_{i=0, \dots, C-1}^T$ measures the probabilistic predictions over C classes. Unlike the conventional PGD- K generating adversarial data by maximizing the loss function ℓ regardless of model prediction, our PGD- K - τ generates the adversarial data which takes model prediction into consideration.

Algorithm 1 returns the misclassified adversarial data with small loss values or correctly classified adversarial data with large loss values. Step τ controls the extent of loss minimization when misclassified adversarial data are found. When τ is larger, the misclassified adversarial data with slightly larger loss values are returned, and vice versa. $\tau \times \alpha$ is an approximation to ρ in our learning objective. Note that when $\tau = K$, the conventional PGD- K is the special case of our PGD- K - τ . As τ is an important hyper-parameter of PGD- K - τ for FAT (Section 5), we discuss in detail how to select τ in Sections 5.1 and 5.2.

4.2 PGD- K - τ Alleviates Cross-over Mixture

In deep neural networks, the cross-over mixture problem may not trivially appear in the original input space, but occur in the output of the intermediate layer. Our proposed PGD- K - τ is an effective solution to overcome this problem, which leads to successful adversarial training.

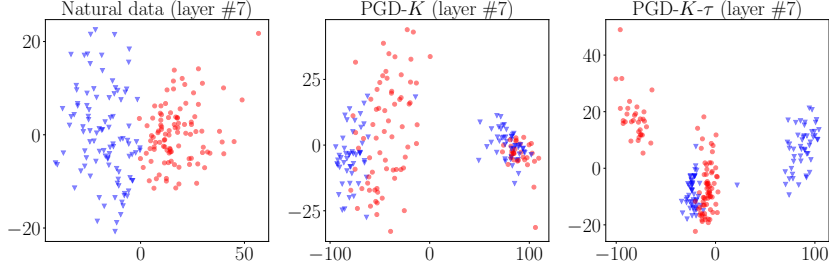


Figure 2: Left: layer #7’s output distribution on natural data (not mixed). Middle: layer #7’s output distribution on adversarial data generated by PGD-20 (significantly mixed). Right: layer #7’s output distribution on friendly adversarial data generated by PGD-20-0 (not significantly mixed).

In Figure 2, we trained an 8-layer convolutional neural network (6 convolutional layers and 2 fully-connected layers) on images of two selected classes in CIFAR-10. We conducted a warm-up training using natural training data, then included their adversarial variants generated by PGD-20 (middle panel) and PGD-20-0 (right panel).

Figure 2 shows the output distribution of layer #7 by principal component analysis (PCA, [33]), which projects high-dimensional output into a two-dimensional subspace. As shown in Figure 2, the output distribution on natural data (left panel) of the intermediate layer is clearly not mixed. By contrast, the conventional PGD- K (middle panel) leads to severe mixing between outputs of adversarial data with different classes. Fitting these mixed adversarial data is more difficult, which leads to inaccurate classifiers. By comparing with PGD- K , our PGD- K - τ (right panel) could largely overcome the mixture issue of adversarial data. Thus, it helps the training algorithm to return an accurate classifier while ensuring adversarial robustness.

To further justify the above fact, we plot output distributions of other layers, e.g., layer #6 and layer #8. Moreover, we train a Wide ResNet (WRN-40-4) [16] on 10 classes and randomly select 3 classes for illustrating their output distributions of its intermediate layers. Instead of PCA, we also use a non-linear technique for dimensionality reduction, i.e., t-distributed stochastic neighbor embedding (t-SNE) [34] to visualize output distributions of different classes. All these can be found in Appendix C.

5 Realization of FAT

Based on the proposed PGD- K - τ , we have a new FAT algorithm (Algorithm 2). FAT treats the standard adversarial training as a special case when we set $\tau = K$ in Algorithm 1. We also design FAT for TRADES (Appendix D.2) and FAT for MART (Appendix E.2). Since the essential component of FAT is PGD- K - τ , we should discuss the effects of step τ w.r.t. standard accuracy and adversarial robustness (Section 5.1) and computational efficiency (Section 5.2). Besides, we should discuss the relation between FAT and curriculum learning (Section 5.3), since FAT is a progressive training strategy.

5.1 Selection of Step τ

As shown in Section 2.2, the conventional PGD- K is a special case, when step $\tau = K$ in PGD- K - τ . Thus, standard adversarial training is a special case of FAT. Here, we investigate how step τ affects the performance of FAT empirically, and summarize that larger τ may not increase adversarial robustness but hurt the standard test accuracy. Detailed experimental setups of Figure 3 are in Appendix F.1.

Figure 3 shows that, with the increase of τ , the standard test accuracy for natural data decreases significantly; while the robust test accuracy for adversarial data increases at smaller values of τ but

Algorithm 2 Friendly Adversarial Training (FAT)

Input: network f_θ , training dataset $S = \{(x_i, y_i)\}_{i=1}^n$, learning rate η , number of epochs T , batch size m , number of batches M

Output: adversarially robust network f_θ

for epoch = 1, ..., T **do**

for mini-batch = 1, ..., M **do**

 Sample a mini-batch $\{(x_i, y_i)\}_{i=1}^m$ from S

for $i = 1, \dots, m$ (in parallel) **do**

 Obtain adversarial data \tilde{x}_i of x_i by Algorithm 1

end for

$\theta \leftarrow \theta - \eta \frac{1}{m} \sum_{i=1}^m \nabla_\theta \ell(f_\theta(\tilde{x}_i), y_i)$

end for

end for

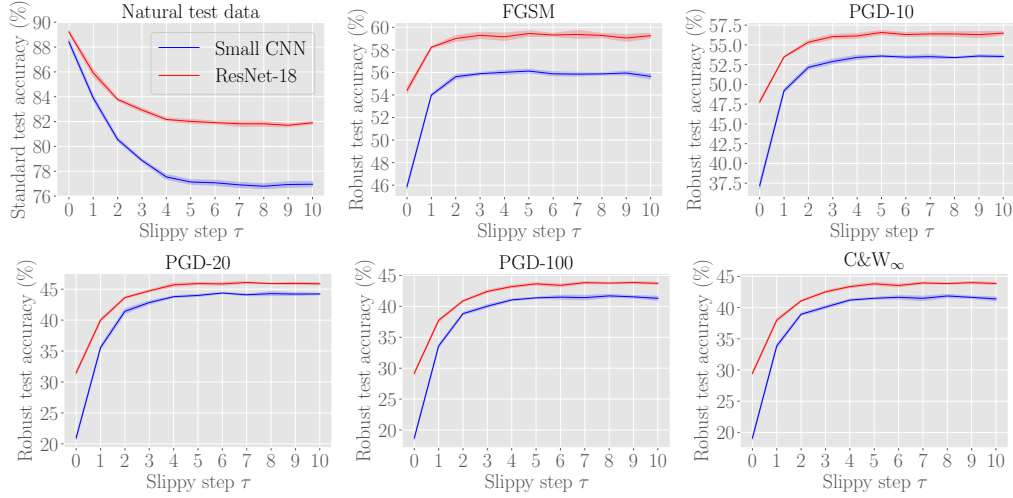


Figure 3: We conduct our adversarial training FAT with various values of step τ on two networks Small CNN (blue line) and ResNet-18 (red line). We evaluate the adversarial training performance according to networks’ standard test accuracy for natural test data and robust test accuracy for adversarial test data generated by FGSM, PGD-10, PGD-20, PGD-100 and C&W attack. We report the median test accuracy and its standard deviation as the shaded color over 5 repeated trials of adversarial training.

reaches its plateau at larger values of τ . For example, when τ is bigger than 2, the standard test accuracy continues to decrease with larger τ . However, the robust test accuracy begins to maintain a plateau for both Small CNN and ResNet-18. Such observation manifests that a larger step τ may not be necessary for adversarial training. Namely, it may not increase adversarial robustness but hurt the standard accuracy. This reflects a trade-off between the standard accuracy and adversarially robust accuracy [19] and suggests that our step τ helps manage this trade-off.

τ can be treated as a hyper-parameter. Based on the observations in Figure 3, it is enough to select τ from the set $\{0, 1, 2, 3\}$. Note that the size of the set is also influenced by step size α and maximum PGD step K . In Section 6.2, we use τ to fine-tune the performance of FAT.

5.2 Smaller τ is Computationally Efficient

Adversarial training is time-consuming since it needs multiple backward propagations (BPs) to produce adversarial data. The time-consuming factor depends on the number of BPs used for generating adversarial data [27, 28, 29].

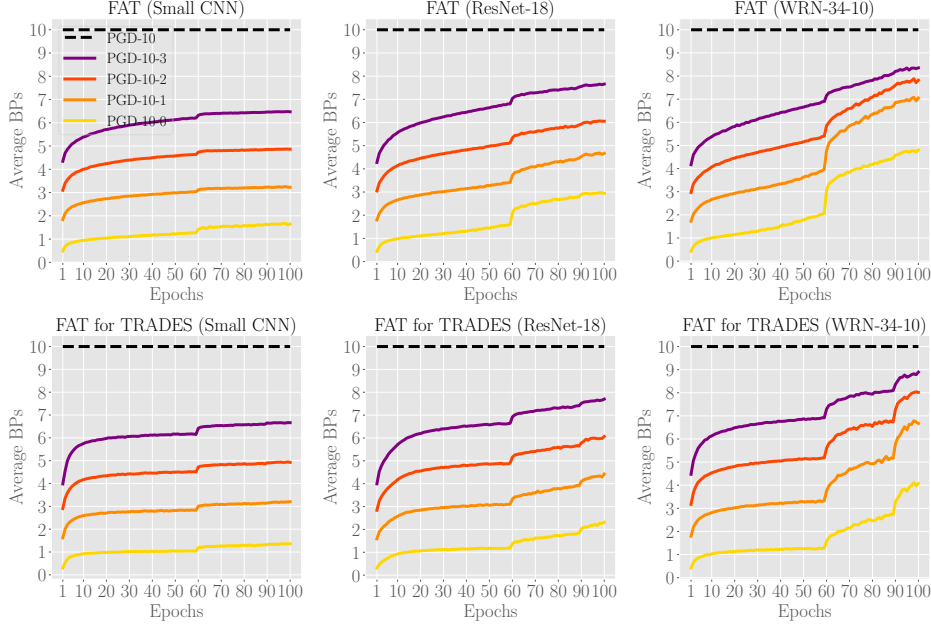


Figure 4: Training statistics on the average number of BPs needed for generating adversarial data. Top three panels are adversarial training FAT on three networks, Small CNN (top left), ResNet-18 (top middle) and WRN-34-10 (top right). Bottom three panels are adversarial training FAT for TRADES on three networks, Small CNN (bottom left), ResNet-18 (bottom middle) and WRN-34-10 (bottom right).

Our FAT uses PGD- K - τ to generate adversarial data, and PGD- K - τ is early-stopped. This implies that FAT is computationally efficient, since FAT does not need to compute maximum K BPs on each mini-batch. To illustrate this, we count the number of BPs for generating adversarial data during training. The training setup is the same as the one in Section 5.1, but we only choose τ from $\{0, 1, 2, 3\}$ and train for 100 epochs with learning rate divided by 10 at epochs 60 and 90. In Figure 4, we compare the standard adversarial training [11] (dashed line) with our FAT (solid line) and adversarial training TRADES [13] (dashed line) with our FAT for TRADES (solid line, detailed in Algorithm 4 in Appendix D.2). For each epoch, we compute average BPs over all training data for generating the adversarial counterpart.

Figure 4 shows that conventional adversarial training uses PGD- K which takes K BPs for generating adversarial data in each mini-batch. By contrast, our adversarial training FAT that uses PGD- K - τ significantly reduces the number of required BPs. In addition, with the smaller τ , FAT needs less BPs on average for generating adversarial data. The magnitude of τ controls the number of extra BPs, once misclassified adversarial data is found.

Moreover, there are some interesting phenomena observed in our FAT (or FAT for TRADES). As the training progresses, the number of BPs gradually increases. This shows that more steps are needed by PGD to find misclassified adversarial data. This signifies that it is increasingly difficult to find adversarial data that misclassifies the model. Thus, DNNs become more and more adversarially robust over training epochs. In addition, there is a slight surge in average BPs at epochs 60 and 90, where we divided the learning rate by 10. This means that the robustness of the model gets substantially improved at epochs 60 and 90. It is a common trick to decrease the learning rate over training DNNs for good standard accuracy [35]. Figure 4 confirms that it is similarly meaningful to decrease the learning rate during adversarial training.

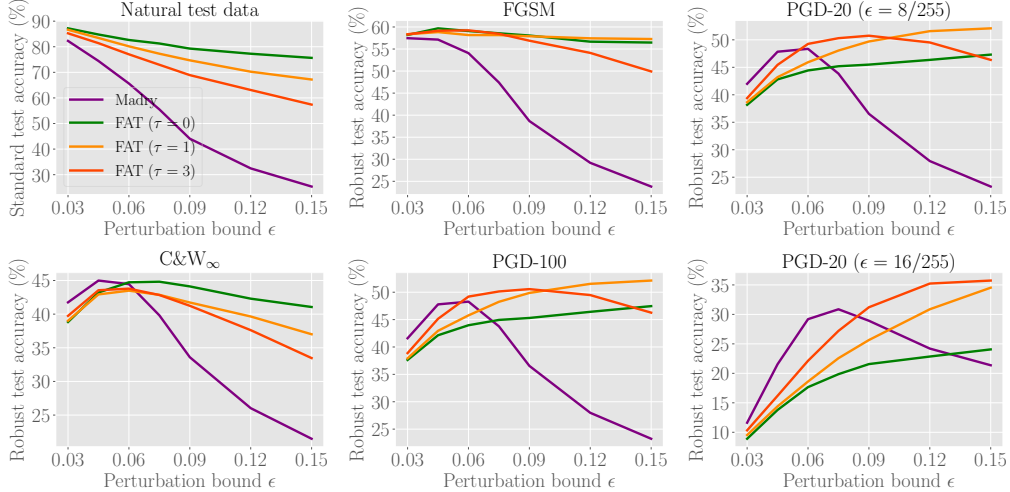


Figure 5: Comparisons on standard test accuracy and robust test accuracy of the deep model (ResNet-18) trained by standard adversarial training (Madry) and our friendly adversarial training ($\tau = 0, 1, 3$) respectively on CIFAR-10 dataset.

5.3 Relation to Curriculum Learning

Curriculum learning [21] is a machine learning strategy that gradually makes the learning task more difficult. Curriculum learning is shown effective in improving standard generalization and providing faster convergence [21].

In adversarial training, curriculum learning can also be used to improve adversarial robustness. Namely, DNNs learn from milder adversarial data first, and gradually adapt to stronger adversarial data. There are different ways to determine the hardness of adversarial data. For example, curriculum adversarial training (CAT) uses the perturbation step K of PGD as the hardness measure [12]. Dynamic adversarial training (DAT) uses their proposed criterion, the first-order stationary condition (FOSC), as the hardness measure [14]. However, both methods do not have a principled way to decide when the hardness should be increased during training. To increase the hardness at the right time, both methods need domain knowledge to fine-tune the curriculum training sequence. For example, CAT needs to decide when to increase step K in PGD over training epochs; while DAT needs to decide FOSC for generating adversarial data at different training stages.

Our FAT can also be regarded as a type of curriculum training. As shown in Figure 4, as the training progresses, more and more BPs are needed to generate adversarial data to fool the classifier. Thus, more and more PGD steps are needed to generate adversarial data. Meanwhile, the network gradually and automatically learns from stronger and stronger adversarial data (adversarial data generated by more and more PGD steps). Differently from CAT and DAT, FAT could automatically increase the hardness of friendly adversarial data based on their model’s predictions of adversarial data. As a result, Table 1 in Section 6.2 shows that empirical results of FAT can outperform the best results in CAT [12], DAT [14] and standard Madry’s adversarial training (not a curriculum learning) [11]. Thus, attacks which do not kill training indeed makes adversarial learning stronger.

6 Experiments

To evaluate the efficacy of FAT, we firstly use CIFAR-10 [36] and SVHN [37] datasets to verify that FAT can help achieve a larger perturbation bound ϵ . Then, we train Wide ResNet [16] on the CIFAR-10 dataset to achieve state-of-the-art results.

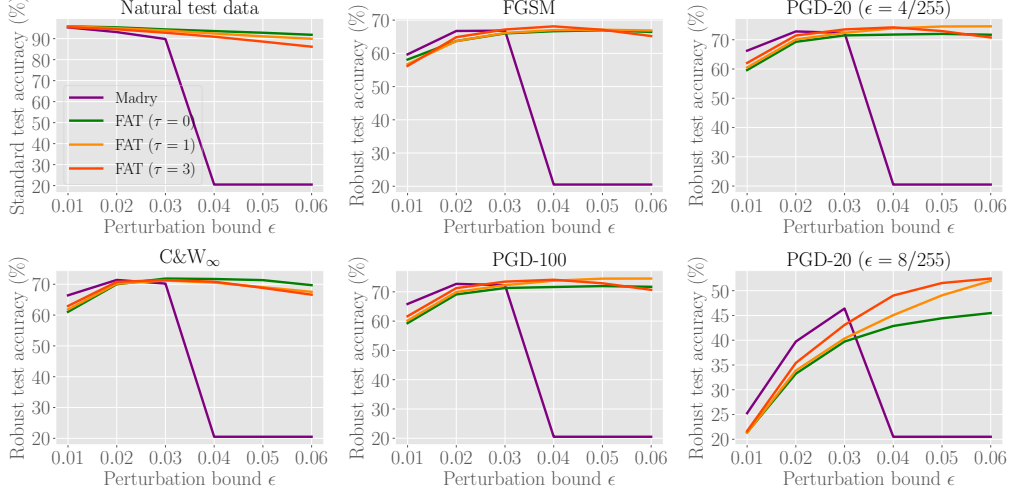


Figure 6: Comparisons on standard test accuracy and robust test accuracy of deep model (ResNet-18) trained by standard adversarial training (Madry) and our friendly adversarial training ($\tau = 0, 1, 3$) respectively on SVHN dataset.

6.1 FAT can Enable Larger Perturbation Bound ϵ

All images of CIFAR-10 and SVHN are normalized into $[0, 1]$. We compare our FAT ($\tau = 0, 1, 3$) and standard adversarial training (Madry) on ResNet-18 with different perturbation bounds ϵ , i.e., $\epsilon \in [0.03, 0.15]$ for CIFAR-10 in Figure 5 and $\epsilon \in [0.01, 0.06]$ for SVHN in Figure 6. The maximum PGD step $K = 10$, step size $\alpha = \epsilon/10$. DNNs were trained using SGD with 0.9 momentum for 80 epochs with the initial learning rate of 0.01 divided by 10 at epoch 60.

In addition, we have experiments of training a different DNN, e.g., Small CNN. We also set maximum PGD step $K = 20$. Besides, we compare our FAT for TRADES and TRADES [13] with different values of ϵ . These extensive results are presented in Appendix G.

Figures 5 and 6 show the performance of FAT ($\tau = 0, 1, 3$) and standard adversarial training w.r.t. standard test accuracy and adversarially robust test accuracy of the DNNs. We obtain standard test accuracy for natural test data and robust test accuracy for adversarial test data. The adversarial test data are bounded by L_∞ perturbations with $\epsilon = 8/255$ for CIFAR-10 and $\epsilon = 4/255$ for SVHN, which are generated by white-box attacks, FGSM, PGD-20, PGD-100 and C&W $_\infty$ (L_∞ version of C&W optimized by PGD-30) [18]. Moreover, we also evaluate the robust DNNs using stronger adversarial test data generated by PGD-20 with a larger perturbation bound $\epsilon = 16/255$ for CIFAR-10 and $\epsilon = 8/255$ for SVHN (bottom right panels in Figures 5 and 6). All PGD attacks have random start, i.e., the uniformly random perturbation of $[-\epsilon, \epsilon]$ added to the natural test data before PGD perturbations. Step size α of PGD is fixed to $2/255$.

From top-left panels of Figures 5 and 6, DNNs trained by FAT ($\tau = 0, 1, 3$) have higher standard test accuracy compared with those trained by standard adversarial training (i.e., Madry). This gap significantly widens as perturbation bound ϵ increases. Larger ϵ will allow the generated adversarial data deviate more from natural data. In standard adversarial training, natural generalization is significantly hurt with larger ϵ due to the cross-over mixture issue. In contrast, DNNs trained by FAT could have better standard generalization, which is less affected by an increasing perturbation bound ϵ .

In addition, with the increase of the perturbation bound ϵ , robust test accuracy (e.g., PGD and C&W) of DNNs trained by standard adversarial training (Madry) gets a slight increase first but is followed by a sharp drop. For a larger ϵ (e.g., $\epsilon > 0.06$ in CIFAR-10 and $\epsilon > 0.03$ in SVHN), standard adversarial training (Madry) basically fails, and thus its robust test accuracy drops sharply. Without early-stopped PGD, the generated adversarial data has a severe cross-over mixture problem, which makes the adversarial learning extremely difficult and sometimes even “kills” the learning.

Table 1: Evaluations (test accuracy) of deep models (WRN-34-10) on CIFAR-10 dataset

Defense	Natural	FGSM	PGD-20	C&W _∞
Madry	87.30	56.10	45.80	46.80
CAT	77.43	57.17	46.06	42.28
DAT	85.03	63.53	48.70	47.27
FAT ($\epsilon = 8/255$)	89.61 ± 0.329	65.19 ± 0.269	46.45 ± 0.448	46.81 ± 0.308
FAT ($\epsilon = 16/255$)	87.02 ± 0.212	65.72 ± 0.296	49.77 ± 0.177	48.59 ± 0.314

Results of Madry, CAT and DAT are reported in [14]. FAT has the same evaluations.

Table 2: Evaluations (test accuracy) of deep models (WRN-34-10) on CIFAR-10 dataset

Defense	Natural	FGSM	PGD-20	C&W _∞
TRADES ($\beta = 1.0$)	88.64	56.38	49.14	-
FAT for TRADES ($\epsilon = 8/255$)	89.94 ± 0.303	61.00 ± 0.418	49.70 ± 0.653	49.35 ± 0.363
TRADES ($\beta = 6.0$)	84.92	61.06	56.61	54.47
FAT for TRADES ($\epsilon = 8/255$)	86.60 ± 0.548	61.97 ± 0.570	55.98 ± 0.209	54.29 ± 0.173
FAT for TRADES ($\epsilon = 16/255$)	84.39 ± 0.030	61.73 ± 0.131	57.12 ± 0.233	54.36 ± 0.177

Results of TRADES ($\beta = 1.0$ and 6.0) are reported in [13]. FAT for TRADES has the same evaluations.

However, it is still meaningful to enable a stronger defense over a weaker attack, i.e., ϵ in adversarial training should be larger than that in adversarial attack. Our friendly adversarial training is able to achieve this. For example, in Figures 5 and 6 our FAT ($\tau = 0, 1, 3$) maintain higher robust accuracy with larger ϵ .

Note that the performance of FAT with PGD-10-3 ($\tau = 3$, red lines) in Figure 5 drops with ϵ larger than 0.09. We believe that FAT with larger τ could have the issue of cross-over mixture, which is detrimental to adversarial learning. In addition, both standard adversarial training and friendly adversarial training do not perform well under C&W attack with larger ϵ (e.g., $\epsilon > 0.075$ in Figure 5), we believe it is due to the mismatch between PGD-adversarial training and C&W attack. We discuss the reasons in detail in Appendix G.4.

To sum up, deep models by FAT with $\tau = 0$ (green line) have higher standard test accuracy, but lower robust test accuracy. By increasing τ to 1, deep models have slightly reduced standard test accuracy but have the increased adversarial robustness. This sheds light on the importance of τ , which handles the trade-off between robustness and standard accuracy. In order not to “kill” the training at the initial stage, we could vary τ from a smaller value to a larger value over training epochs. In addition, due to benefits that our FAT could enable larger ϵ , we could also make ϵ larger over training. Those tricks echo our paper’s philosophy of “attacks which do not kill training make adversarial training stronger”. In the next subsection, we unleash the full power of FAT (and FAT for TRADES) and show its superior performance over state-of-the-art methods.

6.2 Performance Evaluations on Wide ResNet

To manifest the full power of friendly adversarial training, we adversarially train Wide ResNet [16] to achieve the state-of-the-art performance on CIFAR-10. Similar to [14, 13], we employ WRN-34-10 as our deep model.

In Table 1, we compare FAT with standard adversarial training (Madry) [11], CAT [12] and DAT [14] on WRN-34-10. Training and evaluation details are in Appendix H.1. The performance evaluations are done exactly as in DAT [14].

In Table 2, we compare FAT for TRADES with TRADES [13] on WRN-34-10. Training and evaluation details are in Appendix H.2. The performance evaluations are done exactly as in TRADES [13].

Moreover, [38] states that robust classification needs more complex classifiers (exponentially more complex). We employ FAT for TRADES on even larger WRN-58-10, the performance gets improved even more (Appendix H.2). What is more, we also apply the early-stopped PGD to MART, namely, FAT for MART (in Appendix E.2). As a result, the performance gets improved (detailed in Appendix H.3).

Tables 1 and 2 and results in Appendix H justify the efficacy of friendly adversarial training - adversarial robustness can indeed be achieved without compromising the natural generalization. In addition, we are even able to attain the state-of-the-art robustness.

7 Conclusion

This paper proposes a novel friendly adversarial training (FAT). FAT is computationally efficient, and meanwhile, it helps overcome the problem of cross-over mixture. As a result, FAT is able to train deep models with larger perturbation bounds ϵ , and it achieves competitive performance on the large capacity networks. Future potential research includes (a) how to choose optimal step τ in FAT algorithm, (b) besides PGD-K- τ , how to search for friendly adversarial data effectively, (c) and theoretically studying adversarially robust generalization [39], e.g., through the lens of Rademacher complexity [40].

Acknowledgments

This research is supported by the National Research Foundation, Singapore under its Strategic Capability Research Centres Funding Initiative (MK, JZ), JST CREST Grant Number JPMJCR1403 (MS), the National Key R&D Program No.2017YFB1400100, 2017YFB1400102 (LC), HKBU Tier-1 Start-up Grant (HB) and HKBU CSD Start-up Grant (HB). Any opinions, findings and conclusions or recommendations expressed in this material are those of the author(s) and do not reflect the views of National Research Foundation, Singapore.

References

- [1] V. H. Buch, I. Ahmed, and M. Maruthappu, “Artificial intelligence in medicine: current trends and future possibilities,” *Br J Gen Pract*, vol. 68, no. 668, pp. 143–144, 2018.
- [2] T. Litman, *Autonomous vehicle implementation predictions*. Victoria Transport Policy Institute Victoria, Canada, 2017.
- [3] J. M. Cohen, E. Rosenfeld, and J. Z. Kolter, “Certified adversarial robustness via randomized smoothing,” in *Proceedings of the 36th International Conference on Machine Learning, ICML 2019, 9-15 June 2019, Long Beach, California, USA*, 2019, pp. 1310–1320.
- [4] E. Wong and J. Z. Kolter, “Provable defenses against adversarial examples via the convex outer adversarial polytope,” in *Proceedings of the 35th International Conference on Machine Learning, ICML 2018, Stockholmsmässan, Stockholm, Sweden, July 10-15, 2018*, 2018, pp. 5283–5292.
- [5] Y. Tsuzuku, I. Sato, and M. Sugiyama, “Lipschitz-Margin training: Scalable certification of perturbation invariance for deep neural networks,” in *Advances in Neural Information Processing Systems 31: Annual Conference on Neural Information Processing Systems 2018, NeurIPS 2018, 3-8 December 2018, Montréal, Canada*, 2018, pp. 6542–6551.
- [6] M. Lécuyer, V. Atlidakis, R. Geambasu, D. Hsu, and S. Jana, “Certified robustness to adversarial examples with differential privacy,” in *2019 IEEE Symposium on Security and Privacy, SP 2019, San Francisco, CA, USA, May 19-23, 2019*, 2019, pp. 656–672.
- [7] T. Weng, H. Zhang, P. Chen, J. Yi, D. Su, Y. Gao, C. Hsieh, and L. Daniel, “Evaluating the robustness of neural networks: An extreme value theory approach,” in *6th International Conference on Learning Representations, ICLR 2018, Vancouver, BC, Canada, April 30 - May 3, 2018, Conference Track Proceedings*, 2018.
- [8] M. Balunovic and M. Vechev, “Adversarial training and provable defenses: Bridging the gap,” in *International Conference on Learning Representations*, 2020.
- [9] H. Zhang, H. Chen, C. Xiao, S. Gowal, R. Stanforth, B. Li, D. Boning, and C.-J. Hsieh, “Towards stable and efficient training of verifiably robust neural networks,” in *International Conference on Learning Representations*, 2020.
- [10] I. J. Goodfellow, J. Shlens, and C. Szegedy, “Explaining and harnessing adversarial examples,” in *3rd International Conference on Learning Representations, ICLR 2015, San Diego, CA, USA, May 7-9, 2015, Conference Track Proceedings*, 2015.
- [11] A. Madry, A. Makelov, L. Schmidt, D. Tsipras, and A. Vladu, “Towards deep learning models resistant to adversarial attacks,” in *6th International Conference on Learning Representations, ICLR 2018, Vancouver, BC, Canada, April 30 - May 3, 2018, Conference Track Proceedings*, 2018.
- [12] Q. Cai, C. Liu, and D. Song, “Curriculum adversarial training,” in *Proceedings of the Twenty-Seventh International Joint Conference on Artificial Intelligence, IJCAI 2018, July 13-19, 2018, Stockholm, Sweden*, 2018, pp. 3740–3747.
- [13] H. Zhang, Y. Yu, J. Jiao, E. P. Xing, L. E. Ghaoui, and M. I. Jordan, “Theoretically principled trade-off between robustness and accuracy,” in *Proceedings of the 36th International Conference on Machine Learning, ICML 2019, 9-15 June 2019, Long Beach, California, USA*, 2019, pp. 7472–7482.
- [14] Y. Wang, X. Ma, J. Bailey, J. Yi, B. Zhou, and Q. Gu, “On the convergence and robustness of adversarial training,” in *Proceedings of the 36th International Conference on Machine Learning, ICML 2019, 9-15 June 2019, Long Beach, California, USA*, 2019, pp. 6586–6595.

- [15] Y. Wang, D. Zou, J. Yi, J. Bailey, X. Ma, and Q. Gu, “Improving adversarial robustness requires revisiting misclassified examples,” in *International Conference on Learning Representations*, 2020.
- [16] S. Zagoruyko and N. Komodakis, “Wide residual networks,” *arXiv preprint arXiv:1605.07146*, 2016.
- [17] A. Athalye, N. Carlini, and D. A. Wagner, “Obfuscated gradients give a false sense of security: Circumventing defenses to adversarial examples,” in *Proceedings of the 35th International Conference on Machine Learning, ICML 2018, Stockholmsmässan, Stockholm, Sweden, July 10-15, 2018*, 2018, pp. 274–283.
- [18] N. Carlini and D. A. Wagner, “Towards evaluating the robustness of neural networks,” in *2017 IEEE Symposium on Security and Privacy, SP 2017, San Jose, CA, USA, May 22-26, 2017*, 2017, pp. 39–57.
- [19] D. Tsipras, S. Santurkar, L. Engstrom, A. Turner, and A. Madry, “Robustness may be at odds with accuracy,” in *7th International Conference on Learning Representations, ICLR 2019, New Orleans, LA, USA, May 6-9, 2019*, 2019.
- [20] C. Szegedy, W. Zaremba, I. Sutskever, J. Bruna, D. Erhan, I. Goodfellow, and R. Fergus, “Intriguing properties of neural networks,” in *International Conference on Learning Representations*, 2014.
- [21] Y. Bengio, J. Louradour, R. Collobert, and J. Weston, “Curriculum learning,” in *Proceedings of the 26th annual international conference on machine learning*. ACM, 2009, pp. 41–48.
- [22] A. Shamir, I. Safran, E. Ronen, and O. Dunkelman, “A simple explanation for the existence of adversarial examples with small hamming distance,” *arXiv preprint arXiv:1901.10861*, 2019.
- [23] M. Cisse, P. Bojanowski, E. Grave, Y. Dauphin, and N. Usunier, “Parseval networks: Improving robustness to adversarial examples,” in *Proceedings of the 34th International Conference on Machine Learning-Volume 70*. JMLR. org, 2017, pp. 854–863.
- [24] M. Hein and M. Andriushchenko, “Formal guarantees on the robustness of a classifier against adversarial manipulation,” in *Advances in Neural Information Processing Systems*, 2017, pp. 2266–2276.
- [25] Z. Yan, Y. Guo, and C. Zhang, “Deep defense: Training dnns with improved adversarial robustness,” in *Advances in Neural Information Processing Systems*, 2018, pp. 419–428.
- [26] F. Farnia, J. M. Zhang, and D. Tse, “Generalizable adversarial training via spectral normalization,” in *7th International Conference on Learning Representations, ICLR 2019, New Orleans, LA, USA, May 6-9, 2019*, 2019.
- [27] A. Shafahi, M. Najibi, M. A. Ghiasi, Z. Xu, J. Dickerson, C. Studer, L. S. Davis, G. Taylor, and T. Goldstein, “Adversarial training for free!” in *Advances in Neural Information Processing Systems*. Curran Associates, Inc., 2019, pp. 3353–3364.
- [28] D. Zhang, T. Zhang, Y. Lu, Z. Zhu, and B. Dong, “You only propagate once: Accelerating adversarial training via maximal principle,” in *Advances in Neural Information Processing Systems*. Curran Associates, Inc., 2019, pp. 227–238.
- [29] E. Wong, L. Rice, and J. Z. Kolter, “Fast is better than free: Revisiting adversarial training,” in *International Conference on Learning Representations*, 2020.
- [30] Y. Carmon, A. Raghuathan, L. Schmidt, J. C. Duchi, and P. S. Liang, “Unlabeled data improves adversarial robustness,” in *Advances in Neural Information Processing Systems*, 2019, pp. 11 190–11 201.

- [31] A. Najafi, S.-i. Maeda, M. Koyama, and T. Miyato, “Robustness to adversarial perturbations in learning from incomplete data,” in *Advances in Neural Information Processing Systems*, 2019, pp. 5542–5552.
- [32] J. Alayrac, J. Uesato, P. Huang, A. Fawzi, R. Stanforth, and P. Kohli, “Are labels required for improving adversarial robustness?” in *Advances in Neural Information Processing Systems*, 2019, pp. 12 192–12 202.
- [33] H. Abdi and L. J. Williams, “Principal component analysis,” *Wiley interdisciplinary reviews: computational statistics*, vol. 2, no. 4, pp. 433–459, 2010.
- [34] L. v. d. Maaten and G. Hinton, “Visualizing data using t-sne,” *Journal of machine learning research*, vol. 9, no. Nov, pp. 2579–2605, 2008.
- [35] K. He, X. Zhang, S. Ren, and J. Sun, “Deep residual learning for image recognition,” in *Proceedings of the IEEE conference on computer vision and pattern recognition*, 2016, pp. 770–778.
- [36] A. Krizhevsky, “Learning multiple layers of features from tiny images,” Tech. Rep., 2009.
- [37] Y. Netzer, T. Wang, A. Coates, A. Bissacco, B. Wu, and A. Y. Ng, “Reading digits in natural images with unsupervised feature learning,” in *NIPS Workshop on Deep Learning and Unsupervised Feature Learning*, 2011.
- [38] P. Nakkiran, “Adversarial robustness may be at odds with simplicity,” *arXiv preprint arXiv:1901.00532*, 2019.
- [39] D. Yin, K. Ramchandran, and P. L. Bartlett, “Rademacher complexity for adversarially robust generalization,” in *Proceedings of the 36th International Conference on Machine Learning, ICML 2019, 9-15 June 2019, Long Beach, California, USA*, 2019, pp. 7085–7094.
- [40] P. L. Bartlett and S. Mendelson, “Rademacher and gaussian complexities: Risk bounds and structural results,” *Journal of Machine Learning Research*, vol. 3, no. Nov, pp. 463–482, 2002.
- [41] T. Miyato, S. Maeda, M. Koyama, K. Nakae, and S. Ishii, “Distributional smoothing by virtual adversarial examples,” in *4th International Conference on Learning Representations, ICLR*, 2016.

A Friendly Adversarial Training

For completeness, besides the learning objective by loss value, we also give the learning objective of FAT by class probability. Then, based on the learning objective by loss value, we give the proof of Theorem 1, which theoretically justifies FAT.

A.1 Learning Objective

Case 1 (by loss value, restated). The outer minimization still follows Eq. (3). However, instead of generating \tilde{x}_i via inner maximization, we generate \tilde{x}_i as follows:

$$\begin{aligned} \tilde{x}_i &= \arg \min_{\tilde{x} \in \mathcal{B}_\epsilon[x_i]} \ell(f(\tilde{x}), y_i) \\ \text{s.t. } &\ell(f(\tilde{x}), y_i) - \min_{y \in \mathcal{Y}} \ell(f(\tilde{x}), y) \geq \rho. \end{aligned}$$

Note that the operator $\arg \max$ in Eq. (4) is replaced with $\arg \min$ here, and there is a constraint on the margin of loss values (i.e., the mis-classification confidence).

The constraint firstly ensures $y_i \neq \arg \min_{y \in \mathcal{Y}} \ell(f(\tilde{x}), y)$ or \tilde{x} is mis-classified, and secondly ensures for \tilde{x} the wrong prediction is better than the desired prediction y_i by at least ρ in terms of the loss value. Among all such \tilde{x} satisfying the constraint, we select the one minimizing $\ell(f(\tilde{x}), y_i)$. Namely, we minimize the adversarial loss given that a confident adversarial data has been found. This \tilde{x}_i could be regarded as a friend among the adversaries, which is termed as friendly adversarial data.

Case 2 (by class probability). We redefine the above objective from the loss point of view (above) to the class probability point of view. The objective is still Eq. (3), in which $\ell(f(\tilde{x}), y) = \ell_B(\ell_L(f(\tilde{x})), y)$. Hence, $\ell_L(f(\tilde{x}))$ is an estimate of the class-posterior probability $p(y | \tilde{x})$, and for convenience, denote by $p_f(y | \tilde{x})$ the y -th element of the vector $\ell_L(f(\tilde{x}))$.

$$\begin{aligned} \tilde{x}_i &= \arg \max_{\tilde{x} \in \mathcal{B}_\epsilon[x_i]} p_f(y_i | \tilde{x}) \\ \text{s.t. } &\max_{y \in \mathcal{Y}} p_f(y | \tilde{x}) - p_f(y_i | \tilde{x}) \geq \rho. \end{aligned}$$

The constraint ensures \tilde{x} is misclassified by at least ρ , but here the margin ρ is applied to the class probability instead of the loss value. Hence, \tilde{x}_i should usually be different from the one according to the loss value.

A.2 Proofs

We derive a tight upper bound on adversarially robust risk (adversarial risk), and provide our theoretical analysis for the adversarial risk minimization. X and Y represent random variables. Adversarial risk $\mathcal{R}_{\text{rob}}(f) := \mathbb{E}_{(X,Y) \sim \mathcal{D}} \mathbb{1}\{\exists X' \in \mathcal{B}_\epsilon[X] : f(X') \neq Y\}$. $\mathcal{R}_{\text{rob}}(f)$ can be decomposed, i.e., $\mathcal{R}_{\text{rob}}(f) = \mathcal{R}_{\text{nat}}(f) + \mathcal{R}_{\text{bdy}}(f)$, where natural risk $\mathcal{R}_{\text{nat}}(f) = \mathbb{E}_{(X,Y) \sim \mathcal{D}} \mathbb{1}\{f(X) \neq Y\}$ and boundary risk $\mathcal{R}_{\text{bdy}}(f) = \mathbb{E}_{(X,Y) \sim \mathcal{D}} \mathbb{1}\{X \in \mathcal{B}_\epsilon[DB(f)], f(X) = Y\}$. Note that $\mathcal{B}_\epsilon[DB(f)]$ is the set denoting the decision boundary of f , i.e., $\{x \in \mathcal{X} : \exists x' \in \mathcal{B}_\epsilon[x] \text{ s.t. } f(x) \neq f(x')\}$.

Lemma 1. For any classifier $f : \mathcal{X} \rightarrow \mathcal{Y}$, any probability distribution \mathcal{D} on $\mathcal{X} \times \mathcal{Y}$, we have

$$\mathcal{R}_{\text{rob}}(f) = \mathcal{R}_{\text{nat}}(f) + \mathbb{E}_{(X,Y) \sim \mathcal{D}} \mathbb{1}\{\exists X' \in \mathcal{B}_\epsilon[X] : f(X) \neq f(X')\} \cdot \mathbb{1}\{f(X) = Y\}$$

Proof. By the equation $\mathcal{R}_{\text{rob}}(f) = \mathcal{R}_{\text{nat}}(f) + \mathcal{R}_{\text{bdy}}(f)$,

$$\begin{aligned} \mathcal{R}_{\text{rob}}(f) &= \mathcal{R}_{\text{nat}}(f) + \mathcal{R}_{\text{bdy}}(f) \\ &= \mathcal{R}_{\text{nat}}(f) + \mathbb{E}_{(X,Y) \sim \mathcal{D}} \mathbb{1}\{X' \in \mathcal{B}_\epsilon[DB(f)], f(X) = Y\} \\ &= \mathcal{R}_{\text{nat}}(f) + \Pr[X' \in \mathcal{B}_\epsilon[DB(f)], f(X) = Y] \\ &= \mathcal{R}_{\text{nat}}(f) + \Pr[f(X) \neq f(X'), f(X) = Y] \\ &= \mathcal{R}_{\text{nat}}(f) + \mathbb{E}_{(X,Y) \sim \mathcal{D}} \mathbb{1}\{\exists X' \in \mathcal{B}_\epsilon[X] : f(X) \neq f(X'), f(X) = Y\} \\ &= \mathcal{R}_{\text{nat}}(f) + \mathbb{E}_{(X,Y) \sim \mathcal{D}} \mathbb{1}\{\exists X' \in \mathcal{B}_\epsilon[X] : f(X) \neq f(X')\} \cdot \mathbb{1}\{f(X) = Y\} \end{aligned}$$

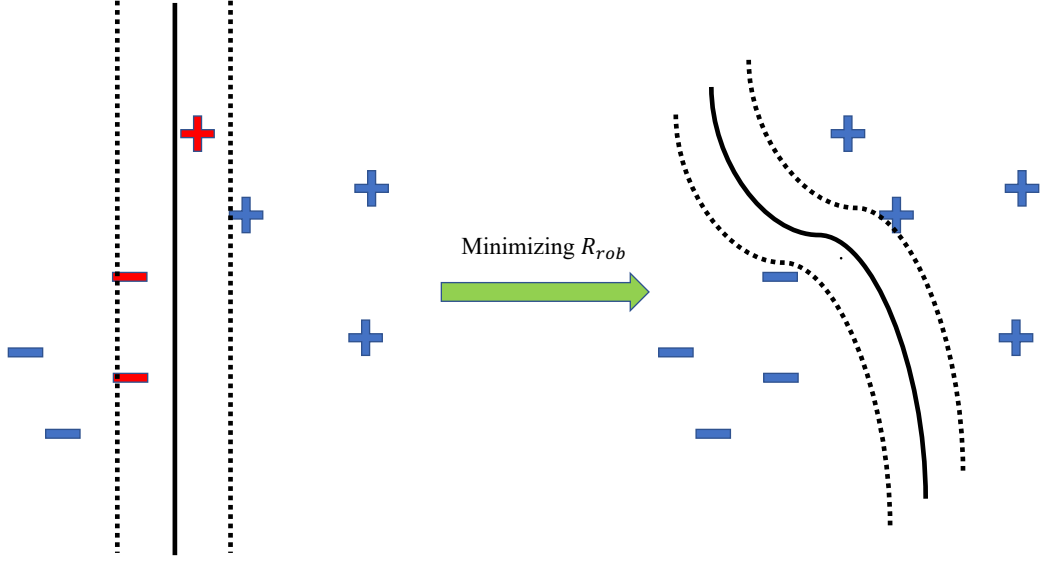


Figure 7: Solid line is the classifier. The area between dashed line is decision boundary of the classifier. Minimizing robust risk R_{rob} is to find a classifier, where data is less likely located within decision boundary of the classifier.

The fourth equality comes from the definition of decision boundary of f , i.e., $\mathcal{B}_\epsilon[DB(f)] = \{x \in \mathcal{X} : \exists x' \in \mathcal{B}_\epsilon[x] \text{ s.t. } f(x) \neq f(x')\}$. \square

Figure 7 illustrates the message of Lemma 1. Minimizing robust risk R_{rob} encourages the learning algorithm to find a classifier whose decision boundary contains less training data. Meanwhile, the classifier should correctly separate data from different classes. Finding such a classifier is hard. As we can see in Figure 7, the hypothesis set of hyperplanes is enough for minimizing the natural risk (the left figure). However, a robust classifier (the right figure) has much curvatures, which is more complicated. [38] states that robust classification needs more complex classifiers (exponentially more complex, in some examples). This implies that in order to learn a robust classifier, our learning algorithm needs (a) setting a large hypothesis set and (b) fine-tuning the decision boundary.

Theorem 1 (restated). For any classifier f , any non-negative surrogate loss function ℓ which upper bounds 0/1 loss, and any probability distribution \mathcal{D} , we have

$$\mathcal{R}_{\text{rob}}(f) \leq \underbrace{\mathbb{E}_{(X,Y) \sim \mathcal{D}} \ell(f(X), Y)}_{\text{For standard test accuracy}} + \underbrace{\mathbb{E}_{(X,Y) \sim \mathcal{D}, X' \in \mathcal{B}_\epsilon[X, \epsilon]} \ell^*(f(X'), Y)}_{\text{For robust test accuracy}},$$

where

$$\ell^* = \begin{cases} \min \ell(f(X'), Y) + \rho, & \text{if } f(X') \neq Y; \\ \max \ell(f(X'), Y), & \text{if } f(X') = Y. \end{cases}$$

ρ is the small constant.

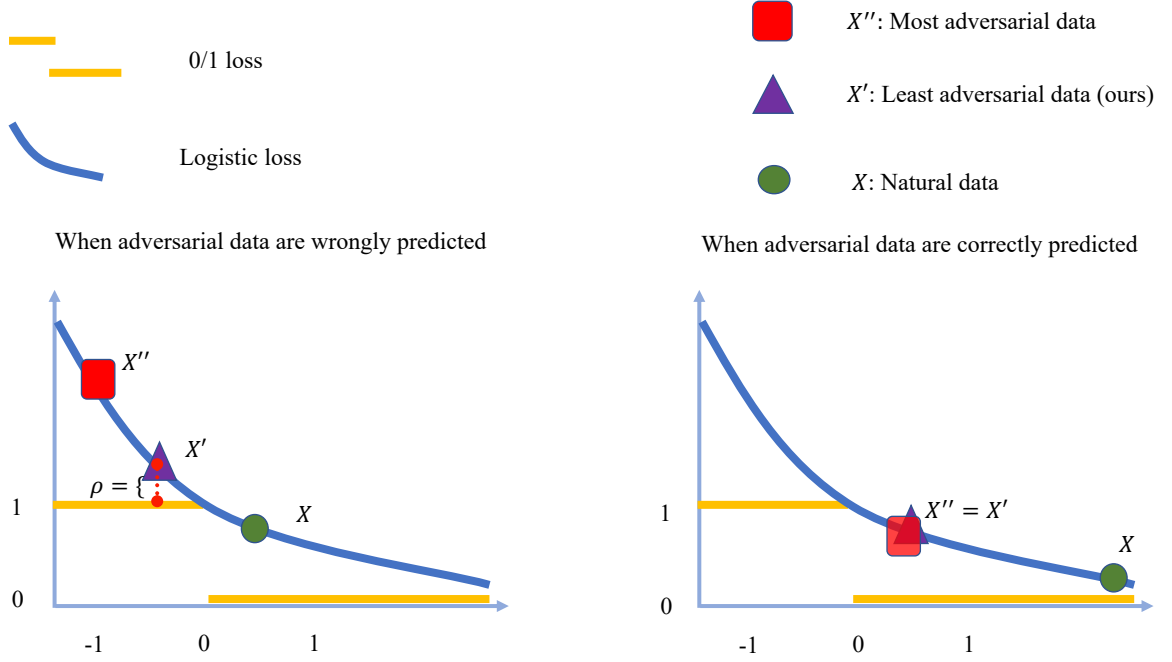


Figure 8: Given a classifier f , in adversarial training, the adversarial data is generated within the perturbation ball $\mathcal{B}_\epsilon[X]$ of natural data X . The current adversarial training generates adversarial data X'' that maximizes the inner loss regardless of its prediction. Ours takes its prediction into account. When the classifier makes the wrong prediction of adversarial data, our least adversarial data X' minimizes the inner loss by a violation of a small constant ρ .

Proof.

$$\begin{aligned}
\mathcal{R}_{\text{rob}}(f) &= \mathcal{R}_{\text{nat}}(f) + \mathcal{R}_{\text{bdy}}(f) \\
&\leq \mathbb{E}_{(X,Y) \sim \mathcal{D}} \ell(f(X), Y) + \mathcal{R}_{\text{bdy}}(f) \\
&= \mathbb{E}_{(X,Y) \sim \mathcal{D}} \ell(f(X), Y) + \mathbb{E}_{(X,Y) \sim \mathcal{D}} \mathbb{1}\{X \in \mathcal{B}_\epsilon[DB(f)], f(X) = Y\} \\
&= \mathbb{E}_{(X,Y) \sim \mathcal{D}} \ell(f(X), Y) + \Pr[X \in \mathcal{B}_\epsilon[DB(f)], f(X) = Y] \\
&= \mathbb{E}_{(X,Y) \sim \mathcal{D}} \ell(f(X), Y) + \Pr[f(X) \neq f(X'), f(X) = Y] \\
&\leq \mathbb{E}_{(X,Y) \sim \mathcal{D}} \ell(f(X), Y) + \Pr[f(X') \neq Y] \\
&= \mathbb{E}_{(X,Y) \sim \mathcal{D}} \ell(f(X), Y) + \mathbb{E}_{(X,Y) \sim \mathcal{D}} \mathbb{1}\{\exists X' \in \mathcal{B}_\epsilon[X] : f(X') \neq Y\} \\
&\leq \mathbb{E}_{(X,Y) \sim \mathcal{D}} \ell(f(X), Y) + \mathbb{E}_{(X,Y) \sim \mathcal{D}, X' \in \mathcal{B}_\epsilon[X, \epsilon]} \ell^*(f(X'), Y)
\end{aligned}$$

The first inequality comes from the assumption that surrogate loss function ℓ upper bound 0/1 loss function. The second inequality comes from the fact that there exists misclassified natural data within the decision boundary set. Therefore, $\Pr[f(X) \neq f(X'), f(X) = Y] \cup \Pr[f(X) \neq f(X'), f(X) \neq Y] = \Pr[f(X') \neq Y]$. The third inequality comes from the assumption that surrogate loss function ℓ upper bound 0/1 loss function, i.e., in Figure 8, the adversarial data X' (purple triangle) is on line of logistic loss (blue line), which is always above the 0/1 loss (yellow line). \square

Our Theorem 1 informs our strategy to fine tune the decision boundary. To fine-tune the decision boundary, the data “near” the classifier plays an important role. Those data are easily wrongly predicted with small perturbations. As we show in the Figure 8, when adversarial data are wrongly predicted, our adversarial data (purple triangle) increases to minimize the loss by a violation of a

small constant ρ . Thus, our adversarial data can help fine-tune the decision boundary “bit by bit” over the training.

B Alternative Adversarial Data Searching Algorithm

In this section, we give an alternative adversarial data searching algorithm to generate friendly adversarial data via modifying the method to update \tilde{x} in Algorithm 1. We remove the constraint of ϵ -ball projection in Eq. (5), i.e.,

$$x^{(t+1)} = x^{(t)} + \alpha \text{sign}(\nabla_{x^{(t)}} \ell(f_{\theta}(x^{(t)}), y)), \forall t \geq 0 \quad (6)$$

where x^0 is a natural data and $\alpha > 0$ is step size.

We employ Small CNN and ResNet-18 to show the performance of deep models against FGSM, PGD-20, PGD-100 and C&W $_{\infty}$ in Figure 9 and Figure 10. Deep models are trained using SGD with 0.9 momentum for 80 epochs with the initial learning rate 0.01 divided by 10 at 60 epoch. We compare FAT combined with the alternative adversarial data searching algorithm ($\tau = 0, 1, 3$) and standard adversarial training (Madry) with different step size α , i.e., $\alpha \in [0.003, 0.015]$. The maximum PGD step K is fixed to 10. All the testing settings are the same as those are stated in Section 6.1.

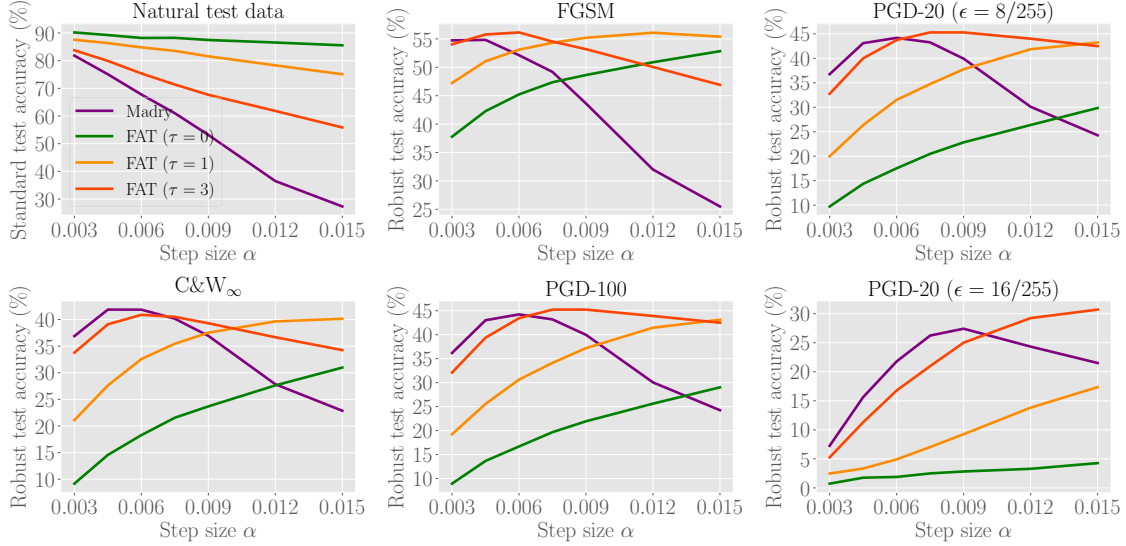


Figure 9: Test accuracy of Small CNN trained under different step size α on CIFAR-10

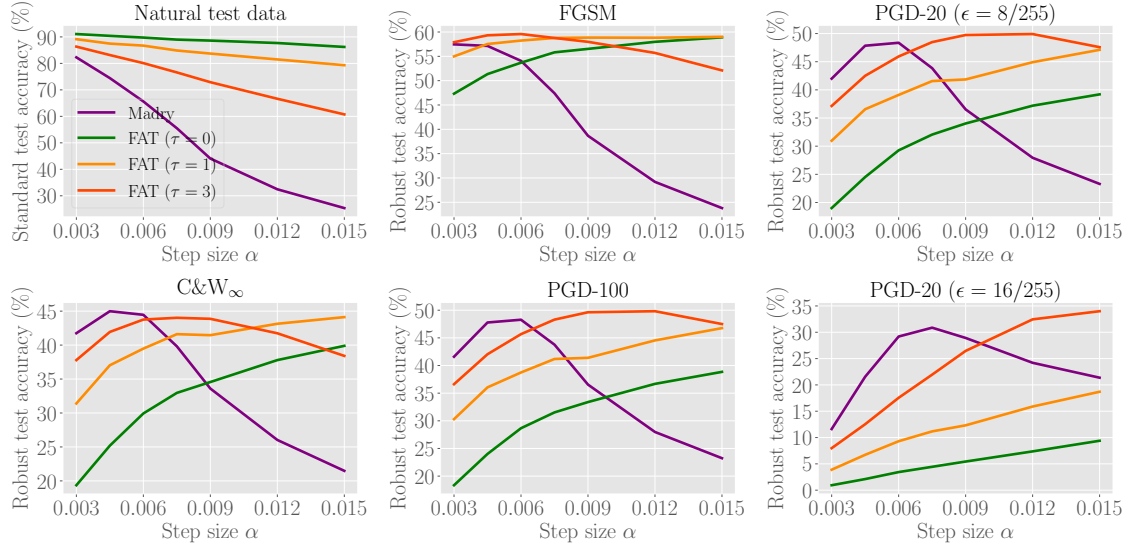


Figure 10: Test accuracy of ResNet-18 trained under different step size α on CIFAR-10

C Mixture Alleviation

C.1 Output Distributions of Small CNN’s Intermediate Layers

In Figure 2 in Section 4.2, we only visualize layer #7’s output distribution by Small CNN (8-layer convolutional neural network with 6 convolutional layers and 2 fully connected layers). For completeness, we visualize the output distributions of layers #7 and #8.

We conduct warm-up training using natural training data of two randomly selected classes (bird and deer) in CIFAR-10, then involve its adversarial variants generated by PGD-20 with step size $\alpha = 0.007$ and maximum perturbation $\epsilon = 0.031$. We show output distributions of layer #6, #7 and #8 by PCA in Figure 11(a) and t-SNE in Figure 11(b).

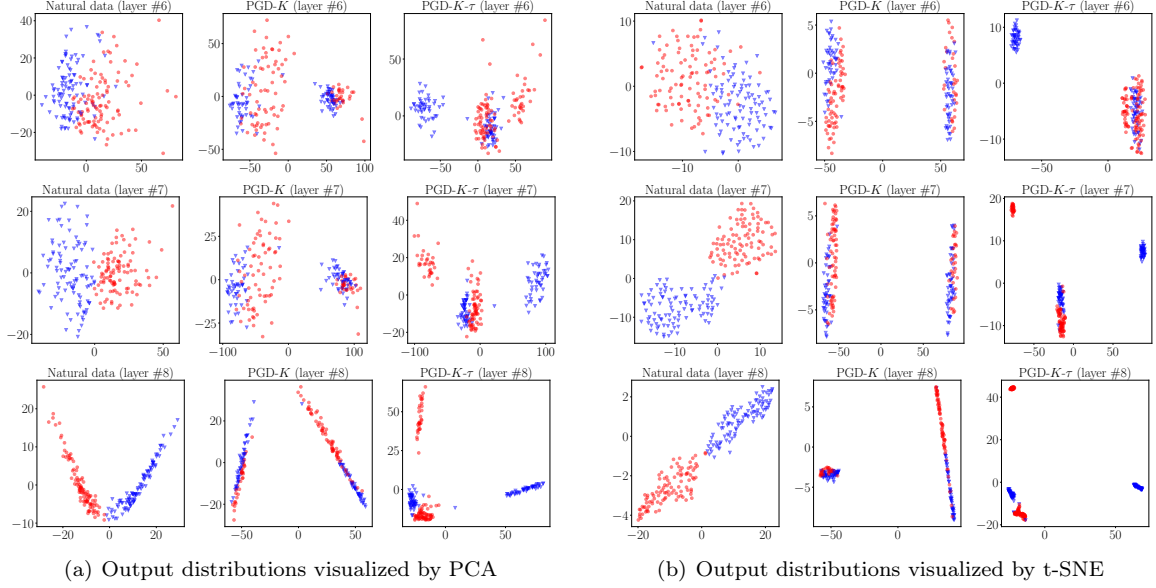


Figure 11: Output distributions of Small CNN’s intermediate layers. Left column: Intermediate layers’ output distributions on natural data (not mixed). Middle column: Intermediate layers’ output distributions on adversarial data generated by PGD-20 (significantly mixed). Right column: Intermediate layers’ output distributions on friendly adversarial data generated by PGD-20-0 (no significantly mixed).

C.2 Output distributions of WRN-40-4’s intermediate layers

We train a Wide ResNet (WRN-40-4, totally 41 layers) using natural data on 10 classes in CIFAR-10 and then include adversarial variants. We randomly select 3 classes (deer, horse and truck) for illustrating output distributions of WRN-40-4’s intermediate layers. Adversarial data are generated by PGD-20 with step size $\alpha = 0.007$ and maximum perturbation $\epsilon = 0.031$ on WRN-40-4. We show output distributions by layer #38, #40 and #41 by PCA in Figure 12(a) and t-SNE in Figure 12(b).

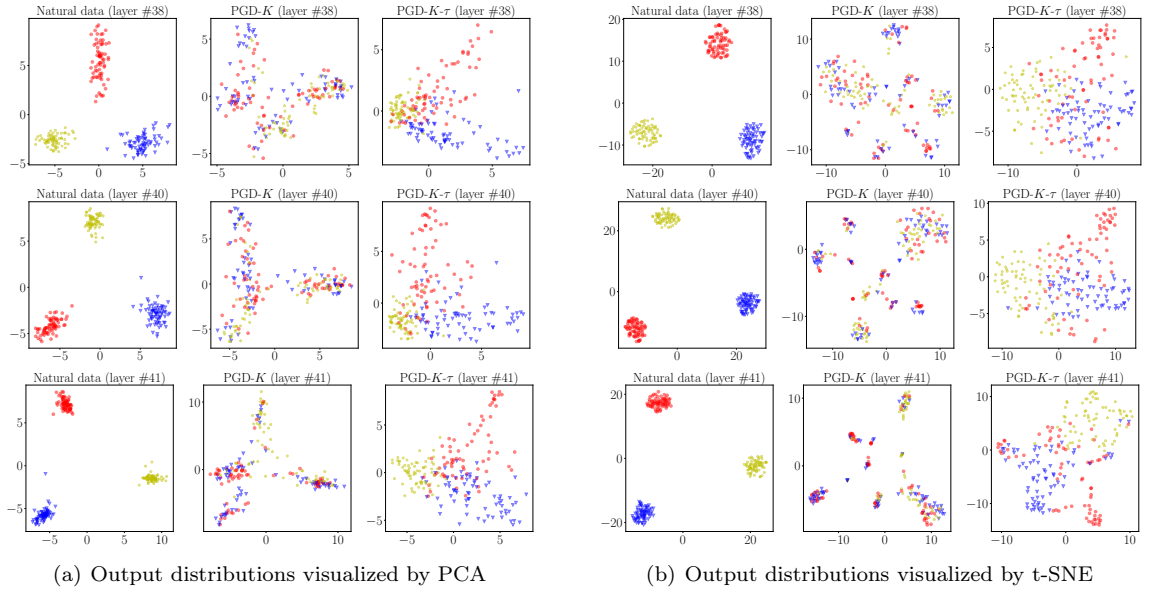


Figure 12: Output distributions of WRN-40-4’s intermediate layers. Left column: Intermediate layers’ output distributions on natural data (not mixed). Middle column: Intermediate layers’ output distributions on adversarial data generated by PGD-20 (significantly mixed). Right column: Intermediate layers’ output distributions on friendly adversarial data generated by PGD-20-0 (no significantly mixed).

D FAT for TRADES

D.1 Learning Objective of TRADES

Besides the standard adversarial training, TRADES is another effective adversarial training method [13], which trains on both natural data x and adversarial data \tilde{x} .

Similar to virtual adversarial training (VAT) adding a regularization term to the loss function [41], which regularizes the output distribution by its local sensitivity of the output w.r.t. input, the objective of TRADES is

$$\min_{f \in \mathcal{F}} \frac{1}{n} \sum_{i=1}^n \left\{ \ell(f(x_i), y_i) + \beta \ell_{KL}(f(\tilde{x}_i), f(x_i)) \right\}, \quad (7)$$

where $\beta > 0$ is a regularization parameter, which controls the trade-off between standard accuracy and robustness accuracy, i.e., as β increases, standard accuracy will decrease while robustness accuracy will increase, and vice visa. Meanwhile, \tilde{x}_i in TRADES is dynamically generated by

$$\tilde{x}_i = \arg \max_{\tilde{x} \in \mathcal{B}_\epsilon[x_i]} \ell_{KL}(f(\tilde{x}), f(x)), \quad (8)$$

and ℓ_{KL} is Kullback-Leibler loss that is calculated by

$$\ell_{KL}(f(\tilde{x}), f(x)) = \sum_{i=1}^C \ell_L^i(f(x)) \log \left(\frac{\ell_L^i(f(x))}{\ell_L^i(f(\tilde{x}))} \right).$$

D.2 FAT for TRADES - Realization

Algorithm 3 PGD- K - τ (Early Stopped PGD for TRADES)

Input: data $\mathbf{x} \in \mathcal{X}$, label $y \in \mathcal{Y}$, model f , loss function ℓ_{KL} , maximum PGD step K , step τ , perturbation bound ϵ , step size α

Output: $\tilde{\mathbf{x}}$

$\tilde{\mathbf{x}} \leftarrow \mathbf{x} + \xi \mathcal{N}(\mathbf{0}, \mathbf{I})$

while $K > 0$ **do**

if $\arg \min_i f(\tilde{\mathbf{x}}) \neq y$ and $\tau = 0$ **then**

break

else if $\arg \min_i f(\tilde{\mathbf{x}}) \neq y$ **then**

$\tau \leftarrow \tau - 1$

end if

$\tilde{\mathbf{x}} \leftarrow \Pi_{\mathcal{B}[\mathbf{x}, \epsilon]}(\alpha \text{sign}(\nabla_{\tilde{\mathbf{x}}} \ell_{KL}(f(\tilde{\mathbf{x}}), f(\mathbf{x}))) + \tilde{\mathbf{x}})$

$K \leftarrow K - 1$

end while

In Algorithm 3, $\mathcal{N}(\mathbf{0}, \mathbf{I})$ generates a random unit vector of d dimension. ξ is a small constant. ℓ_{KL} is Kullback-Leibler loss.

Given a dataset $S = \{(\mathbf{x}_i, y_i)\}_{i=1}^n$, where $\mathbf{x}_i \in \mathcal{R}^d$ and $y_i \in \{0, 1, \dots, C-1\}$, adversarial training (TRADES) with early stopped PGD- K - τ returns a classifier θ^* :

$$\theta^* = \arg \min_{\theta} \sum_{i=1}^n \left\{ \ell_{CE}(f_{\theta}(\mathbf{x}_i), y_i) + \beta \ell_{KL}(f_{\theta}(\tilde{\mathbf{x}}_i), f_{\theta}(\mathbf{x}_i)) \right\} \quad (9)$$

where $f_{\theta} : \mathcal{R}^d \rightarrow \mathcal{R}^C$ is DNN classification function, $f_{\theta}(\cdot)$ outputs predicted probability over C classes, The adversarial data $\tilde{\mathbf{x}}_i$ of \mathbf{x}_i is dynamically generated according to Algorithm 3, $\beta > 0$ is a regularization parameter, ℓ_{CE} is cross-entropy loss, ℓ_{KL} is Kullback-Leibler loss.

Based on our early stopped PGD- K - τ for TRADES in Algorithm 3, our friendly adversarial training for TRADES (FAT for TRADES) is

Algorithm 4 Friendly Adversarial Training for TRADES (FAT for TRADES)

Input: network f_θ , training dataset $S = \{(x_i, y_i)\}_{i=1}^n$, learning rate η , number of epochs T , batch size m , number of batches M
Output: adversarially robust network f_θ
for epoch = 1, \dots , T **do**
 for mini-batch = 1, \dots , M **do**
 Sample a mini-batch $\{(x_i, y_i)\}_{i=1}^m$ from S
 for $i = 1, \dots, m$ (in parallel) **do**
 Obtain adversarial data \tilde{x}_i of x_i by Algorithm 3
 end for
 $\theta \leftarrow \theta - \eta \frac{1}{m} \sum_{i=1}^m \nabla_\theta [\ell_{BCE}(f_\theta(\tilde{x}_i), y_i) + \beta \ell_{KL}(f_\theta(\tilde{\mathbf{x}}_i), f_\theta(\mathbf{x}_i))]$
 end for
end for

E FAT for MART

E.1 Learning Objective of MART

MART [15] emphasizes the importance of misclassified natural data on the adversarial robustness. It proposes a regularized adversarial learning objective which contains an explicit differentiation of misclassified data as the regularizer. The learning objective of MART is

$$\min_{f \in \mathcal{F}} \frac{1}{n} \sum_{i=1}^n \left\{ \ell_{BCE}(f(\tilde{x}_i), y_i) + \beta \cdot \ell_{KL}(f(\tilde{x}_i), f(x_i)) \cdot (1 - \ell_L^{y_i}(f(x_i))) \right\}, \quad (10)$$

where $\beta > 0$ is a regularization parameter which balances the two parts of the final loss. ℓ_{KL} is Kullback-Leibler loss. ℓ_L^k stands for the k -th element of the soft-max output and \tilde{x}_i in MART is dynamically generated according to Eq. 4 that is realized by PGD-K. The first part ℓ_{BCE} is the proposed BCE loss in MART that is calculated by

$$\ell_{BCE}(f(\tilde{x}_i), y_i) = -\log(\ell_L^{y_i}(f(\tilde{x}_i))) - \log(1 - \max_{k \neq y_i} \ell_L^k(f(\tilde{x}_i)))$$

where the first term $-\log(\ell_L^{y_i}(f(\tilde{x}_i)))$ is the cross-entropy loss and the second term $-\log(1 - \max_{k \neq y_i} \ell_L^k(f(\tilde{x}_i)))$ is a margin term used to increase the distance between $\ell_L^{y_i}(f(\tilde{x}_i))$ and $\max_{k \neq y_i} \ell_L^k(f(\tilde{x}_i))$. This is similar to C&W [18] attack that is to improve attack strength. For the second part, they combine Kullback-Leibler loss [13] and emphases on misclassified examples. This part of loss will be large for misclassified examples and small for correctly classified examples.

E.2 FAT for MART - Realization

Given a dataset $S = \{(\mathbf{x}_i, y_i)\}_{i=1}^n$, where $\mathbf{x}_i \in \mathcal{R}^d$ and $y_i \in \{0, 1, \dots, C-1\}$, FAT for MART returns a classifier θ^* :

$$\theta^* = \arg \min_{\theta} \sum_{i=1}^n \left\{ \ell_{BCE}(f_\theta(\tilde{\mathbf{x}}_i), y_i) + \beta \cdot \ell_{KL}(f_\theta(\tilde{\mathbf{x}}_i), f_\theta(\mathbf{x}_i)) \cdot (1 - \ell_L^{y_i}(f_\theta(\mathbf{x}_i))) \right\} \quad (11)$$

where $f_\theta : \mathcal{R}^d \rightarrow \mathcal{R}^C$ is DNN classification function, $f_\theta(\cdot)$ outputs predicted probability over C classes. The adversarial data $\tilde{\mathbf{x}}_i$ of \mathbf{x}_i is dynamically generated according to Algorithm 1, ℓ_L is the soft-max activation, $\beta > 0$ is a regularization parameter, ℓ_{BCE} is the proposed BCE loss in MART and ℓ_{KL} is Kullback-Leibler loss. Based on our early stopped PGD-K- τ in Algorithm 1, FAT for MART Algorithm 5.

Algorithm 5 Friendly Adversarial Training for MART (FAT for MART)

Input: network f_θ , training dataset $S = \{(x_i, y_i)\}_{i=1}^n$, learning rate η , number of epochs T , batch size m , number of batches M
Output: adversarially robust network f_θ
for epoch = 1, \dots , T **do**
 for mini-batch = 1, \dots , M **do**
 Sample a mini-batch $\{(x_i, y_i)\}_{i=1}^m$ from S
 for $i = 1, \dots, m$ (in parallel) **do**
 Obtain adversarial data \tilde{x}_i of x_i by Algorithm 1
 end for
 $\theta \leftarrow \theta - \eta \frac{1}{m} \sum_{i=1}^m \nabla_\theta [\ell_{BCE}(f_\theta(\tilde{x}_i), y_i) + \beta \cdot \ell_{KL}(f_\theta(\tilde{x}_i), f_\theta(x_i)) \cdot (1 - \ell_L^{y_i}(f_\theta(x_i)))]$
 end for
end for

F Experimental Setup

F.1 Selection of Step τ

Figure 3 presents empirical results on CIFAR-10 via our FAT algorithm, where we train 8-layer convolutional neural network (Small CNN, blue line) and 18-layer residual neural network (ResNet-18, red line) [35]. The maximum step $K = 10$, $\epsilon = 8/255$, step size $\alpha = 0.007$, and step $\tau \in \{0, 1, \dots, 10\}$. We train deep networks for 80 epochs using SGD with 0.9 momentum, where learning rate starts at 0.1 and divided by 10 at 60 epoch.

For each τ , we take five trials, where each trial will obtain standard test accuracy evaluated on natural test data and robust test accuracy evaluated on adversarial test data that are generated by attacks FGSM [10], PGD-10 and PGD-20, PGD-100 [11] and C&W attack [18] respectively. All those attacks are white box attacks, which are constrained by the same perturbation bound $\epsilon = 8/255$. Following [13], all attacks have the random start, and the step size α in PGD-10, PGD-20, PGD-100 and C&W is fixed to 0.003.

G Supplementary Experiments - FAT Enabling Larger ϵ

In this section, we provide extensive experimental results. The test settings are the same as those are stated in Section 6.1. In Section G.1, instead of using ResNet-18, we conduct adversarial training on the deep model of Small CNN. In Section G.2, instead of applying FAT, we compare our FAT for TRADES and TRADE [13] under different values of perturbation bound ϵ on the deep models ResNet-18 and Small CNN. In Section G.3, we set maximum PGD steps $K = 20$ and report results of FAT and FAT for TRADES over existing methods with larger perturbation bound ϵ . To sum up, all those extensive results verify that FAT and FAT for TRADES can enable deep models trained under larger values of perturbation bound ϵ .

G.1 A Different Deep Model - Small CNN

We train Small CNN on CIFAR-10 and SVHN using the same settings as those stated in Section 6.1. We show standard and robust test accuracy of deep model (Small CNN) on CIFAR-10 dataset (Figure 13) and SVHN dataset (Figure 14).

G.2 FAT for TRADES

We apply FAT for TRADES (Algorithm 4) to Small CNN and ResNet-18 on CIFAR-10 dataset. All training settings are the same as those are stated in Section 6.1. Regularization parameter $\beta = 6$. We present standard and robust test results of Small CNN (Figure 15) and ResNet-18 (Figure 16).

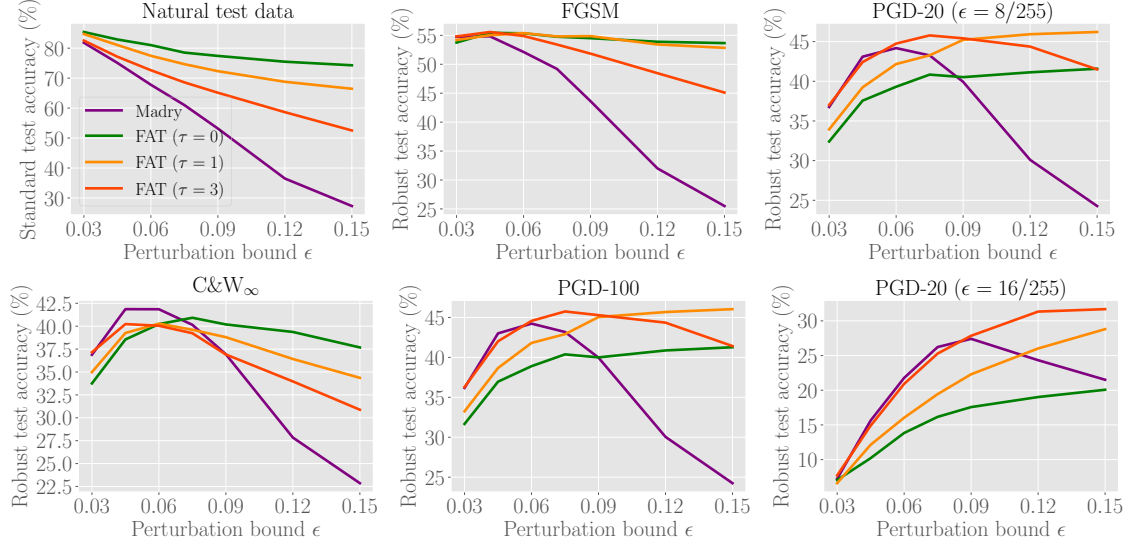


Figure 13: Test accuracy of Small CNN trained under different values of ϵ on CIFAR-10 dataset.

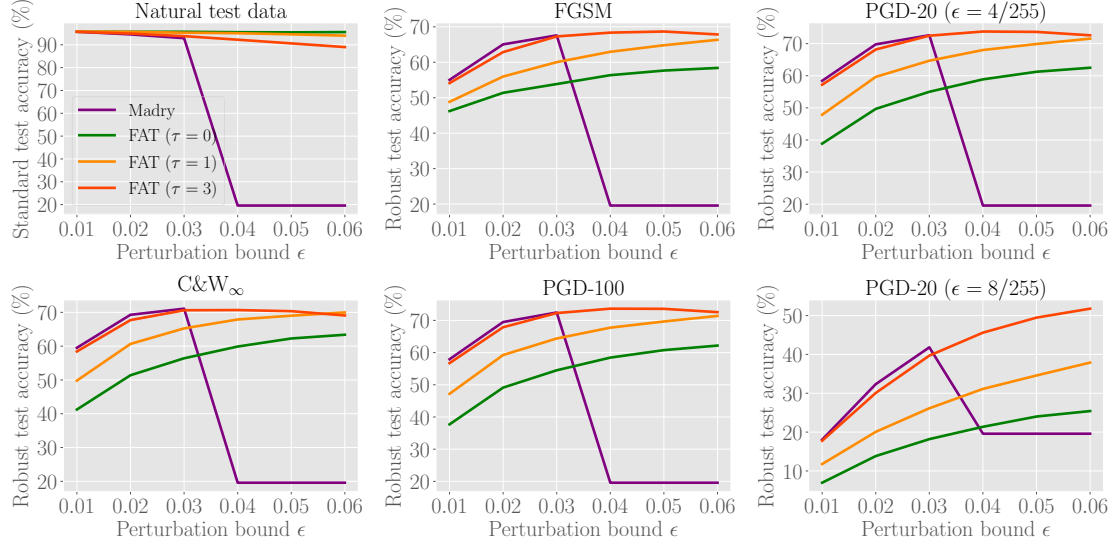


Figure 14: Test accuracy of Small CNN trained under different values of ϵ on SVHN dataset.

G.3 Maximum PGD Step $K = 20$

By setting maximum PGD step $K = 20$, we conduct more experiments on Small CNN and ResNet-18 using FAT and FAT for TRADES. Except maximum PGD steps $K = 20$, training settings are the same as those are stated in Section 6.1. Test results of robust deep models are shown in Figure 17 and Figure 18. Figure 19 and Figure 20.

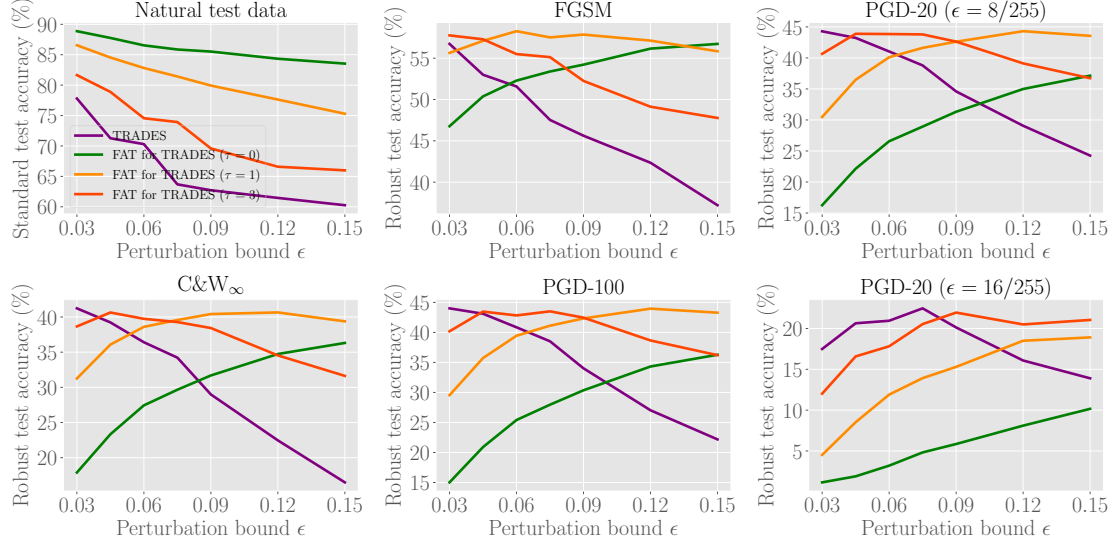


Figure 15: Test accuracy of Small CNN trained by FAT for TRADES ($\tau = 0, 1, 3$) and TRADES under different values of ϵ on CIFAR-10 dataset.

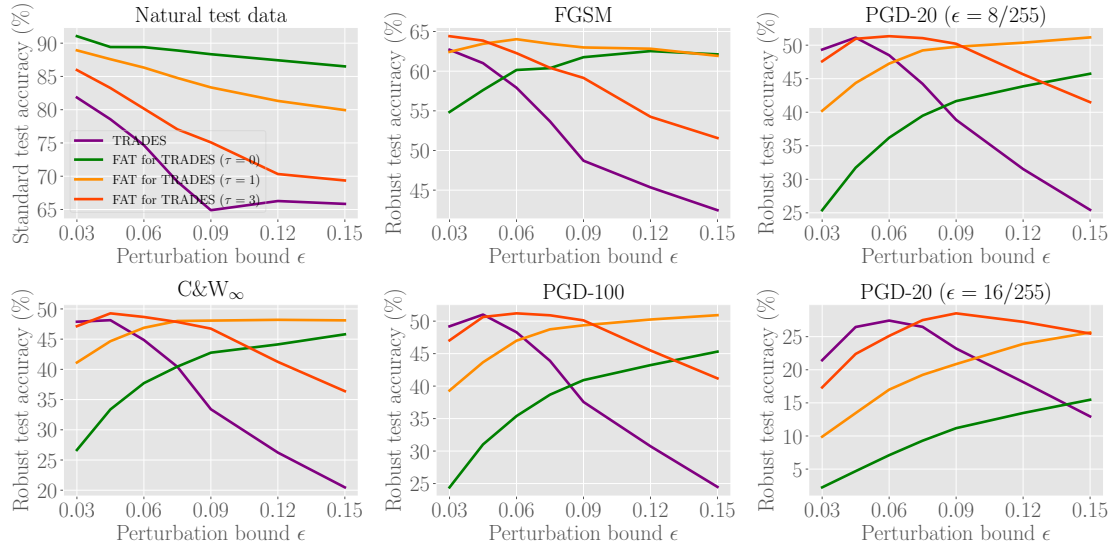


Figure 16: Test accuracy of ResNet-18 trained by FAT for TRADES ($\tau = 0, 1, 3$) and TRADES under different values of ϵ on CIFAR-10 dataset.

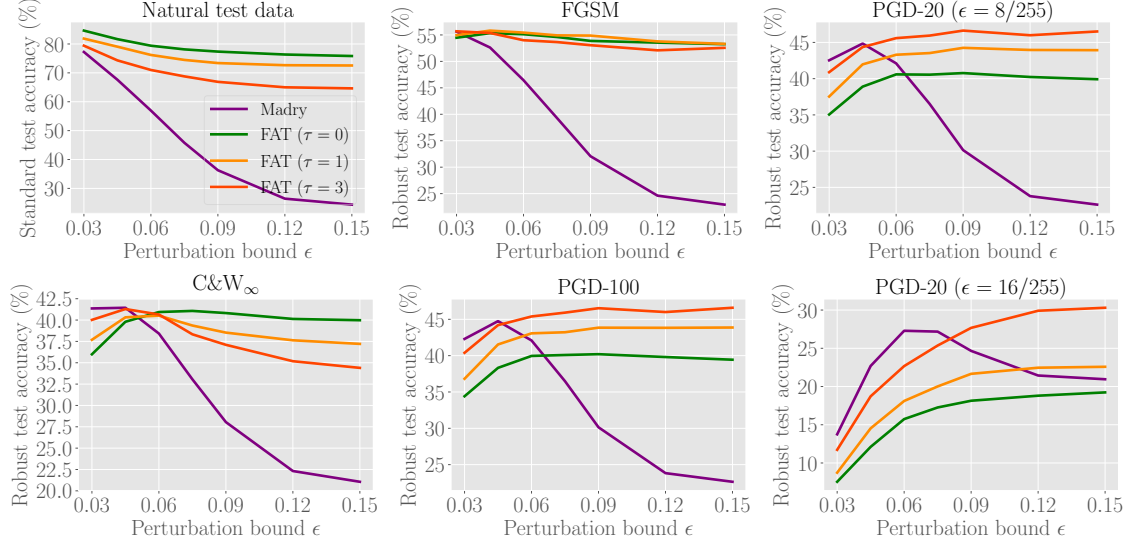


Figure 17: Test accuracy of Small CNN trained by FAT and standard adversarial training (Madry) with maximum PGD step $K = 20$ under different values of ϵ on CIFAR-10 dataset.

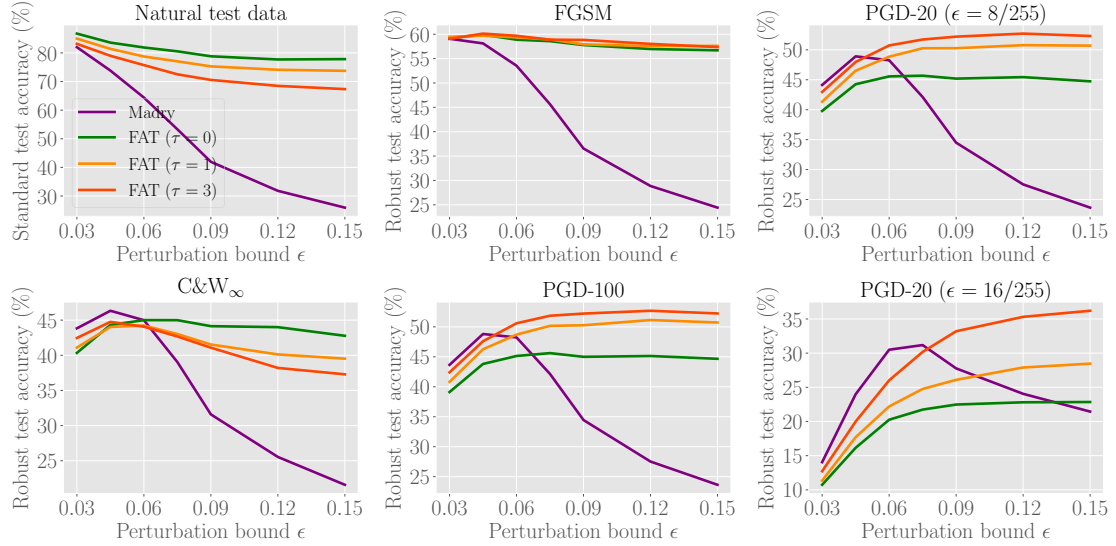


Figure 18: Test accuracy of ResNet-18 trained by FAT standard adversarial training (Madry) with maximum PGD step $K = 20$ under different values of ϵ on CIFAR-10 dataset.

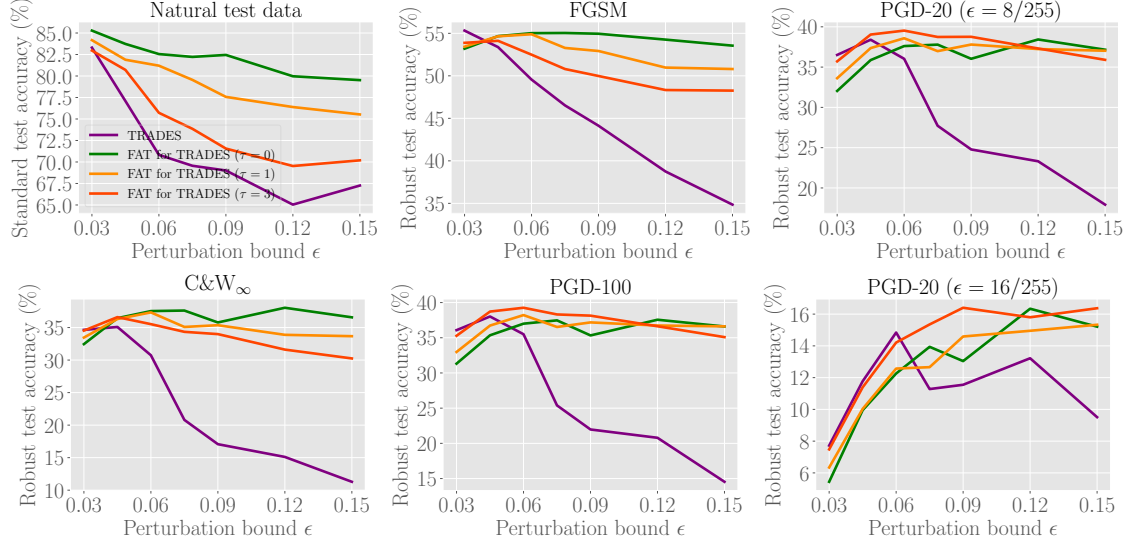


Figure 19: Test accuracy of Small CNN trained by FAT for TRADES and TRADES with maximum PGD step $K = 20$ under different values of ϵ on CIFAR-10 dataset.

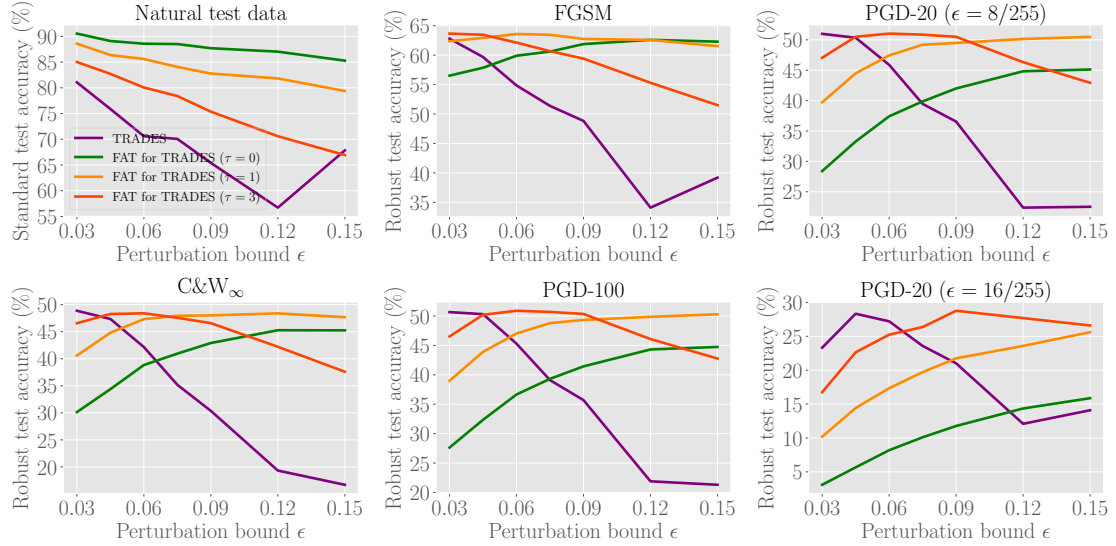


Figure 20: Test accuracy of ResNet-18 trained by FAT for TRADES and TRADES with maximum PGD step $K = 20$ under different values of ϵ on CIFAR-10 dataset.

G.4 C&W Attack Analysis

As is shown in Figure 5 along with Figure 13 in Section G.1, both standard adversarial training and friendly adversarial training do not perform well under C&W [18] attack with larger ϵ (e.g., $\epsilon > 0.075$). We discuss the reasons for these phenomena.

C&W attack. Given x , we choose a target class t and then search for adversarial data \tilde{x} under C&W attack in the L_p metric by solving

$$\text{minimize } \|\tilde{x} - x\|_p + c \cdot h(\tilde{x})$$

with h defined as

$$h(\tilde{x}) = \max(\max_{i \neq t} f(\tilde{x})_i - f(\tilde{x})_t, -\kappa).$$

The parameter $c > 0$ balances two parts of loss. $\kappa > 0$ encourages the solver to find adversarial data \tilde{x} that will be classified as class t with high confidence. Note that this paper follows the implementation of C&W_∞ attack in [12]¹ and [14]² where they replace the cross-entropy loss with $h(\tilde{x})$ in PGD, i.e.,

$$\tilde{x}_i = \arg \max_{\tilde{x} \in \mathcal{B}_\epsilon[x_i]} (\max_{i \neq y_i} f(\tilde{x})_i - f(\tilde{x})_{y_i} - \kappa). \quad (12)$$

Analysis. In Figure 5, with larger ϵ , the performance evaluated by PGD attacks increases, while performance evaluated by C&W attack decreases. The reason is that C&W and PGD have different ways of generating adversarial data according to Eq. (12) and Eq. (4) respectively. The two interactive methods search adversarial data in different directions due to gradients w.r.t. different loss. Therefore, the distributions of C&W and PGD adversarial data are inconsistent. As perturbation bound ϵ increases, there are more PGD adversarial data generated within ϵ -ball. A DNN learned from more PGD adversarial data becomes more defensive to PGD attacks, but this deep model may not effectively defend C&W adversarial data.

¹curriculum adversarial training GitHub

²dynamic adversarial training GitHub

H Extensive State-of-the-art Results on Wide ResNet

H.1 Training Details of FAT on WRN-34-10

In Table 1, we compare our FAT with standard adversarial training (Madry), CAT [12] and DAT [14].

We use FAT ($\epsilon = 8/255$ and $16/255$ respectively) to train WRN-34-10 for 120 epochs using SGD with 0.9 momentum, and weight decay is 0.0002. Maximum PGD step is 10 and step size is fixed to 0.007. The initial learning rate is 0.1 reduced to 0.01, 0.001 and 0.0005 at epoch 60, 90 and 110. We set step $\tau = 0$ initially and increase τ by one at epoch 50 and 90 respectively. The maximum step $K = 10$. We report performance of the deep model at the last epoch. For fair comparison, in Table 1 we use the same test settings as those in DAT [14]. Performance of robust deep model is evaluated standard test accuracy for natural data and robust test accuracy for adversarial data, that are generated by FGSM, PGD-20 (20-steps PGD with random start) and C&W $_{\infty}$ (L_{∞} version of C&W optimized by PGD-30).

All attacks have the same perturbation bound $\epsilon = 0.031$ and step size in PGD is $\alpha = \epsilon/4$. The same as DAT [14], there is random start in PGD attack, i.e., uniformly random perturbations $([-\epsilon, +\epsilon])$ added to natural data before PGD perturbations. We report the median test accuracy and its standard deviation over 5 repeated trails of adversarial training in Table 1.

H.2 Training details of FAT for TRADES on Wide ResNet

In Table 2, we use FAT for TRADES ($\epsilon = 8/255$ and $16/255$ respectively) train WRN-34-10 by FAT for TRADES for 85 epochs using SGD with 0.9 momentum and 0.0002 weight decay. Maximum PGD step $K = 10$ and step size $\alpha = 0.007$. The initial learning rate is 0.1 and divided 10 at epoch 75. We set step $\tau = 0$ initially and increased by one at epoch 30, 50 and 70. Since TRADES has a trade-off parameter β , for fair comparison, our FAT for TRADES use the same β . In Table 2, we set $\beta = 1$ and 6 separately, which are endorsed by [13].

For fair comparison, we use the same test settings as those are stated in TRADES [13]. All attacks have the same perturbation bound $\epsilon = 0.031$ (without random start), and step size $\alpha = 0.003$, which is the same as stated in the paper [13]. Performance of robust deep model is evaluated standard test accuracy for natural data and robust test accuracy for adversarial data, that are generated by FGSM, PGD-20 and C&W $_{\infty}$ (L_{∞} version of C&W optimized by PGD-30). We report the median test accuracy and its standard deviation of the deep model at the last epoch over 3 repeated trials of adversarial training in Table 2.

Fair comparison based on TRADES’s experimental setting. However, in TRADES’s experimental testing³, they use random start before PGD perturbation that is deviated from the statements in the paper [13]. For fair comparison, we also retest the robust deep models under PGD attacks with random start. We evaluate their publicly released robust deep model⁴ WRN-34-10 and compare it with ours trained by FAT for TRADES. The test results are reported in Table 3.

FAT for TRADES on larger WRN-58-10. We employ Wide ResNet with larger capacity, i.e., WRN-58-10 to show our superior performance achieved by FAT for TRADES in Table 3. All the training settings are the same as details on WRN-34-10 in this section. The regularization parameter β is fixed to 6.0. All attacks have the same perturbation bound $\epsilon = 0.031$ and step size $\alpha = 0.003$, which is the same as TRADES’s experimental setting. Robustness against FGSM, PGD-20(20-steps PGD with random start) and C&W $_{\infty}$ is reported in Table 3.

H.3 FAT for MART on Wide ResNet

We train WRN-34-10 by FAT for MART ($\epsilon = 8/255$ and $16/255$ respectively) using SGD with 0.9 momentum and 0.0002 weight decay. Maximum PGD step $K = 10$ and step size $\alpha = 0.007$. The

³TRADES GitHub

⁴TRADES’s pre-trained model

Table 3: Robustness (test accuracy) of deep models on CIFAR-10 dataset (evaluated with random start)

Model	Defense	Natural	FGSM	PGD-20	C&W _∞
WRN-34-10	TRADES ($\beta = 6.0$)	84.92	67.00	57.18	54.72
	FAT for TRADES ($\epsilon = 8/255$)	86.38 ± 0.548	67.64 ± 0.572	56.65 ± 0.262	54.51 ± 0.299
	FAT for TRADES ($\epsilon = 16/255$)	84.39 ± 0.030	67.38 ± 0.370	57.67 ± 0.198	54.62 ± 0.140
WRN-58-10	FAT for TRADES ($\epsilon = 8/255$)	87.09	68.7	57.17	55.43
	FAT for TRADES ($\epsilon = 16/255$)	85.28	68.08	58.39	55.89

initial learning rate is 0.1 and divided 10 at epoch 60 and 90 respectively. We set step $\tau = 0$ initially and increase τ by one at epoch 20, 40, 60 and 80. The regularization parameter β is fixed to 6.0. The maximum step size $K = 10$.

Since MART has not released their best model so far, we reproduced the MART’s training strategy according to experimental settings stated in [15]. We train WRN-34-10 by MART using SGD with momentum 0.9, weight decay 0.0002 and an initial rate of 0.1, which is divided by 10 at the 75-th epoch and 90-th epoch (100 epoch in total). The perturbation bound $\epsilon = 8/255$ and parameter $\beta = 6$. Adversarial data generated for updating current model are generated by PGD-10 with random start and step size $\alpha = \epsilon/4$. We achieve MART’s best model at the epoch right after the first time learning rate decay (i.e., epoch 76), which is a trick stated in [15]. In Table 4, we report the best results we achieved.

Fair comparison based on MART’s experimental setting. For fair comparison, all attacks have the same perturbation bound $\epsilon = 8/255$ and step size $\alpha = \epsilon/10$, which is the same setting in MART [15]. White-box robustness of the deep model against attacks such as FGSM, PGD-20 (20-steps PGD with random start) and C&W_∞ (L_∞ version of C&W optimized by PGD-30) is reported. In Table 4, we report the median test accuracy and its standard deviation over 3 repeated trails of FAT for MART on WRN-34-10.

FAT for MART on larger WRN-58-10. In Table 4, we also employ WRN-58-10 to show the performance achieved by FAT for MART. All the training and testing settings are the same as those on WRN-34-10.

Table 4: Robustness (test accuracy) of deep models on CIFAR-10 dataset

Model	Defense	Natural	FGSM	PGD-20	C&W _∞
WRN-34-10	MART ($\beta = 6.0$)	83.51	67.45	57.75	53.60
	FAT for MART ($\epsilon = 8/255$)	86.40 ± 0.071	68.94 ± 0.195	57.89 ± 0.144	52.28 ± 0.110
	FAT for MART ($\epsilon = 16/255$)	84.39 ± 0.390	68.52 ± 0.297	59.13 ± 0.180	52.85 ± 0.459
WRN-58-10	FAT for MART ($\epsilon = 8/255$)	87.10	69.52	58.57	52.73
	FAT for MART ($\epsilon = 16/255$)	85.19	69.00	59.82	53.01